Deep–Sea Research II xxx (xxxx) xxx

Contents lists available at ScienceDirect

Deep-Sea Research Part II

journal homepage: www.elsevier.com/locate/dsr2

Deep-sea acorn worms (Enteropneusta) from the Bering Sea with the description of a new genus and a new species of Torquaratoridae dominating soft-bottom communities☆

Olga Vladimirovna Ezhova [a,*], Anastasiya Ivanovna Lukinykh [a], Sergey Vladimirovich Galkin [b], Elena Mikhailovna Krylova [b], Andrey Viktorovich Gebruk [b]

[a] Lomonosov Moscow State University, Biological Faculty, Department of Invertebrate Zoology, Moscow, 119234, Russia
[b] Shirshov Institute of Oceanology, Russian Academy of Sciences, Moscow, 117997, Russia

ARTICLE INFO

Keywords:
Hemichordata
Morphology
Ecology
Phylogenetic analysis
16S rRNA
Quatuoralisia malakhovi
Harrimaniidae
Saxipendium
Methane seep
Remotely operated vehicle
Photograph *in situ*

ABSTRACT

Five species of deep-sea acorn worms (Enteropneusta) were found in the Bering Sea during cruises of the RV *Akademik M.A. Lavrentyev* in 2016, 2018, and 2021. The worms were recorded on slopes of the Volcanologists Massif and in the Komandorsky Graben at depths between 1830 and 4278 m and on the Koryak slope between 419 and 662 m. Four of the species were only photographed but not collected; these were an unidentified Torquaratoridae gen. sp. 1 and three harrimaniids: *Saxipendium* sp., Harrimaniidae gen. sp. 1 and Harrimaniidae gen. sp. 2. Harrimaniidae gen. sp. 1 and gen. sp. 2 were recorded on the Koryak slope in the vicinity of methane seeps. The fifth species was photographed *in situ* and collected. It has been examined using morphological and molecular methods. It is described in the present study as *Quatuoralisia malakhovi* n. gen. n. sp. Ezhova et Lukinykh (fam. Torquaratoridae). The abundance of this species in the soft-sediment community at the depth 1830–2290 m was up to 12 specimens per m^2, the highest ever recorded for any deep-sea enteropneusts. Morphologically, *Q. malakhovi* n. gen. n. sp. is noteworthy for the mesocoel ducts, the heart-kidney complex with a pericardial coelom, the two-plated skeleton supporting the proboscis stalk, and conspicuously elongated lateral wings developed on either side of the trunk. The molecular analysis based on the mitochondrial 16S rRNA showed that *Q. malakhovi* n. gen. n. sp. is closest to several torquaratorid species that have yet to be formally described morphologically.

1. Introduction

Enteropneusts, or acorn worms, are solitary hemichordates distributed world-wide from the littoral to hadal zone. Traditionally enteropneusts received much attention since it is an important group for understanding of early evolution of the phylum Chordata (Lowe et al., 2006; Miyamoto and Wada, 2013). However, the knowledge was mainly limited by shallow-water representatives and until recently enteropneusts were considered as predominantly costal inhabitants. Because of very fragile and gelatinous bodies, enteropneusts are easily macerated during sampling by traditional deep-sea sampling gear – trawls and grabs. New page in the investigation of acorn worms has begun with development of under-water photography and sampling using remotely operated vehicles (Woodwick and Sensenbaugh, 1985; Hessler et al., 1988; Smith et al., 2005; Holland et al., 2005, 2009; Anderson et al., 2011; Osborn et al., 2012; Priede et al., 2012). Despite still insufficient knowledge of this taxon, the evidence is growing that deep-sea enteropneusts are a morphologically diverse group, playing an important role

Abbreviations: AML, RV *Akademik M.A. Lavrentyev*; IORAN, Shirshov Institute of Oceanology, Russian Academy of Sciences, Moscow, Russia; MAR, Mid-Atlantic Ridge; MIMB, Museum of the A.V. Zhirmunsky Institute of Marine Biology, Far Eastern Branch of the Russian Academy of Sciences, Vladivostok, Russia; MSU, Lomonosov Moscow State University, Moscow, Russia; NSCMB FEB RAN, National Scientific Center of Marine Biology, Far Eastern Branch of Russian Academy of Sciences, Vladivostok, Russia; ROV, remotely operated vehicle.

☆ Supporting grants: Grant of Russian Science Foundation (RSF), project № 18-74-10025, Grant of Russian Foundation for Basic Research (RFBR), project № 20-04-00909-a, Grant of the Ministry of Science and Higher Education, Russian Federation (No 13.1902.21.0012, contract No 075-15-2020-796).

* Corresponding author. Moscow, Leninskie Gory, 1, Bld 12, MSU, 119234, Russia.
E-mail address: olga.ejova@gmail.com (O.V. Ezhova).

https://doi.org/10.1016/j.dsr2.2021.105014
Received 1 May 2021; Received in revised form 1 December 2021; Accepted 5 December 2021
Available online 7 December 2021
0967-0645/© 2021 Elsevier Ltd. All rights reserved.

in nutrient cycling and surficial bioturbation in deep-sea ecosystems (Jones et al., 2013).

Observations in nature (Priede et al., 2012; Jones et al., 2013), results of isotopic (Jones et al., 2013) and morpho-functional analyses (Holland et al., 2009) and examining of the gut contents (Ezhova et al., 2021) indicate that enteropneusts are deposit feeders ingesting the surface layer of the sediment. Different species can demonstrate diverse levels of selectivity varying from little or none (Holland et al., 2009) to rather high (Osborn et al., 2013). Some species are able to drift between feeding sites using near-bottom currents and special mucous cocoons which they secrete to facilitate the lift-off into the water column; voiding gut also helps to lift-off (Holland et al., 2009, 2012a; Osborn et al., 2012; Jones et al., 2013). Acorn worms lay down specific faecal trails which mark their foraging patterns; these patterns may be spiral, clockwise or counter-clockwise, or meandering (Smith et al., 2005; Holland et al., 2009; Anderson et al., 2011). Smith et al. (2005) suggested that acorn worms meander when searching for food and form a spiral when feeding in a nutrient-rich area. Priede et al. (2012) discuss that foraging patterns can be more related to the taxon specificity. The trails can be very abundant being a conspicuous feature of a deep-sea landscape (Smith et al., 2005; Anderson et al., 2011).

Estimates of biomass on the Mid-Atlantic Ridge (MAR) suggest that enteropneusts can make up a substantial proportion of wet megafaunal biomass at ~2500 m depth (Jones et al., 2013). Populations of enteropneusts studied so far did not show very high densities (Table 1). The only exception is data from the south-western Bering Sea where densities reached 12 ind m^{-2} at depths 1830–2130 m (Rybakova et al., 2020). For the MAR it was shown that population density of enteropneusts was generally higher in areas with higher carbon flux to the seafloor (Jones et al., 2013). Earlier Hessler et al. (1988) have demonstrated that in the vicinity of the Rose Garden hydrothermal vent field (Galapagos Rift) temporal changes in the abundance of acorn worms were positively correlated with food availability (Hessler et al., 1988); similar correlation was shown for the station M (34°50'N, 123°00'W, 4100 m) in the north-east Pacific (Smith et al., 2005). Hessler et al. (1988) suggested that the diminution of populations of the harrimaniid *Saxipendium coronatum* at Rose Garden was related to decreasing of the flux of nutritious particles as a result of reducing of the vent activity or increasingly effective filtration by mussels (Hessler et al., 1988). At Station M the density of *Tergivelum baldwinae* increased by an order of magnitude within a year following the increase in food supply (Smith et al., 2005). Availability of nutrients also appears to be an important factor shaping the distribution patterns of enteropneusts within the Australian waters (Anderson et al., 2011).

The class Enteropneusta currently includes four families: Ptychoderidae Spengel, 1893, Spengelidae Willey, 1899, Harrimaniidae Spengel, 1902 and Torquaratoridae Holland et al., 2005. Most species in the first three families live in shallow waters with only four exceptions: *Glossobalanus tuscarorae* Belichov, 1971 (Ptychoderidae) is known from 8100 m, *Glandiceps abyssicola* Spengel, 1893 (Spengelidae) – from 4570 m, *Saxipendium coronatum* Woodwick & Sensenbaugh, 1985, and *S. implicatum* Holland et al., 2012 (Harrimaniidae) – from 2478 m and 1675–3225 m (Holland et al., 2012b). The recently established family Torquaratoridae is limited to the deep-sea, it includes mainly epibenthic species living at depths from 350 to 4000 meters (Holland et al., 2005, 2009, 2012b; Osborn et al., 2013). The common use of remotely operated vehicles (ROV) for sampling and observation in the deep-sea research contributed to an increasing knowledge of the torquaratorid diversity. The family at present includes nine described species assigned to the following six genera (Table 2): *Allapasus* Holland, Kuhnz et Osborn, 2012, *Coleodesmium* Osborn, Gebruk, Rogacheva et Holland, 2013, *Tergivelum* Holland, Jones, Ellena, Ruhl et Smith, 2009, *Terminstomo* Jabr et Cameron, 2018, *Torquarator* Holland, Clague, Gordon, Gebruk, Pawson et Vecchione, 2005, *Yoda* Priede, Osborn, Gebruk, Jones, Shale, Rogacheva et Holland, 2012 (Holland et al., 2005, 2009, 2012a; Priede et al., 2012; Osborn et al., 2013; Jabr et al., 2018).

Molecular data are currently available for six described species and four genera – *Allapasus*, *Coleodesmium*, *Tergivelum*, and *Yoda* (Osborn et al., 2013). Also, there are molecular data for two tentatively suggested but not formally described and named genera designated as Genus B (extra-wide-lipped) and Genus C (narrow-lipped) (Priede et al., 2012; Osborn et al., 2013).

During the cruise 75 of the RV *Akademik M.A. Lavrentyev* to the Bering Sea (2016), observations using ROV were made of the deep-sea megafauna communities dominated by torquaratorid enteropneusts of an undescribed genus and species (Galkin and Ivin, 2019; Rybakova et al., 2020). During cruises 82 (2018) and 93 (2021) of *Akademik M.A. Lavrentyev*, more photo and video records of deep-sea enteropneusts were made in the western Bering Sea in different habitats including slopes of the Piip Volcano (Volcanologists Massif) and methane seeps of the Koryak slope (Galkin et al., 2019). Altogether from these records we identified five species of Enteropneusta (Fig. 1) presumably of the two families, Harrimaniidae and Torquaratoridae (Table 3). We were able to collect only one of them, the most abundant torquaratorid species; the four other species were only imaged *in situ*. Previously only shallow-water enteropneust *Saccoglossus mereschkowskii* (Wagner, 1885) (Harrimaniidae) was known from the Bering Sea (Ezhova, 2013).

Here we provide data on records of all deep-sea enteropneust species in the Bering Sea and describe a new species and a new genus of the torquaratorid (*Quatuoralisia malakhovi* n. gen. n. sp. Ezhova et Lukinykh) dominating bathyal soft-sediment communities on the slope of the Volcanologists Massif in the Bering Sea. The morpho-anatomical

Table 1
Maximum densities of torquaratorid species in different regions.

Species	Maximum density	Site	Depth, m	Reference
Tergivelum baldwinae	2 ind. 1000 m^{-2}	Station M, NE Pacific	4100	Smith et al., 2005
Tergivelum baldwinae	9.5 ind. 100 m^{-2}	Off S.Washington–central California, E Pacific	2712–3954	Osborn et al., 2012
Tergivelum cinnabarium	6.50 ± 4.51 ind. 1000 m^{-2}	Mid Atlantic Ridge	2427–2493	Jones et al., 2013
Yoda purpurata	30.50 ± 13.48 ind. 1000 m^{-2}	Mid Atlantic Ridge	2502–2759	Jones et al., 2013
Genus B (extra wide-lipped) sp. 1	4.7 ind. 100 m^{-2}	Off S.Washington–central California, E Pacific	1712–3287	Osborn et al., 2012
Genus B (extra wide-lipped) sp. 2	0.3 ind. 100 m^{-2}	Off S.Washington–central California, E Pacific	1674–2847	Osborn et al., 2012
Genus C (narrow-lipped) sp. 1	0.3 ind. 100 m^{-2}	Off S.Washington–California, E Pacific	2252–3124	Osborn et al., 2012
Mixture of torquaratorid species	29.9 ind. 1000 m^{-2}	Offshore western Australia, E Indian Ocean	2155–2183	Anderson et al., 2011
Mixture of torquaratorid species	17.6 ind. 1000 m^{-2}	Offshore eastern Australia, W Pacific	2053–2073	Anderson et al., 2011
Quatuoralisia malakhovi n. gen. n. sp.	12 ind. m^{-2}	Bering Sea, the Volcanologists Massif	1830–2130	Rybakova et al., 2020; this paper

ARTICLE IN PRESS

Table 2
Comparison of all known Torquaratorids including *Quatuoralisia malakhovi* n. gen. n. sp. (based on Jabr et al., 2018 with additions).

	Allapasus aurantiacus	*Allapasus fuscus*	*Allapasus isidis*	*Coleodesmium karaensis*	*Tergivelum baldwinae*	*Tergivelum cinnabarinum*	*Terminstomo arcticus*	*Torquarator bullocki*	*Yoda purpurata*	*Quatuoralisia malakhovi*
Source	Holland et al., 2012a	Jabr et al., 2018	Priede et al., 2012	Osborn et al., 2013	Holland et al., 2009	Priede et al., 2012	Jabr et al., 2018	Holland et al., 2005	Priede et al., 2012	This paper
Living length, cm	26; 18 (after fixation)	2.92	13	6.3	9	12	2.21	7	12	11.5
- holotype										
- paratypes					up to 28	11–26			13–19	6–17
Living holotype color	Light orange (anterior); light beige (posterior)	Dark brown	Light yellow	Translucent & lightly lavender color	Dark brown (anterior); beige (posterior)	Cinnabar (anterior); pale orange (posterior)	Transparent; white anterior gut; dark pigmented intestine	Tan (anterior); light blue (posterior)	Dark reddish purple	Translucent; banana yellow gonads & light blue posterior half
Proboscis shape	Pointed dome	Short dome	Dome	Dome	Shallow rounded dome	Dome	Dome	Low dome	Smooth dome	Low dome
Proboscis length, cm (holotype)	0.6 (after fixation)	0.32	?	0.9	?	?	0.32	0.5	2	0.4
Proboscis width, cm (holotype)	1 (after fixation)	0.31	?	1.2	?	?	0.51	0.8	3.5	1.3
Proboscis groove	Ventral	Dorsal	Ventral	Dorsal & ventral	No	No	Ventral	No	No	Several short grooves on all sides
Proboscis muscles	Radially	Abundant, dispersed muscle fibers	Similar to *A. aurantiacus*	Loose mesh partly horizontal	Anteroposterior tract & delicate meshwork	Similar to *T. baldwinae*	Poorly developed	Poorly developed	Diffuse	Poorly developed
Presence & shape of proboscis skeleton	Plate (nearly vertical)	No	Plate-like	Tubular	No	No	No	Reduced	No	Two plates
Proboscis skeleton horns	No	No	No	No	No	No	No	Short	No	No
Buccal diverticulum	Yes	Yes	Yes	Yes	No	No	Yes	Yes	No	Yes
Glomerulus	Yes	Yes	Yes	Yes	No	No	Yes	No	No	Yes
Heart	Yes	No	Yes	?	No	No	No	No	No	No
Pericardium	No	No	No	No	No	No	No	No	No	Yes
Buccal cavity	Yes	Yes	Yes	Yes	Yes	Yes	Yes	Yes	No	No
Collar length, cm (holotype)	0.5 (after fixation)	0.28	?	0.5	?	?	0.3	0.7	0.5	0.45–0.55
Collar width, cm (holotype)	1 (after fixation)	0.35	?	1.4	2	?	0.54	1.5	6	2.1
Collar lateral lips	No	No	No	No	Yes	Yes	No	No	Yes	Yes
Collar midventral lip	No	No	No	No	Yes	No	No	No	Yes	Yes
Buccal muscles	?	?	?	?	Yes	Yes	?	?	?	Yes
Proboscis or mesocoel pores	No	No	No	No	No	No	No	?	No	Yes
Trunk length, cm (holotype)	17 (after fixation)	2.32	?	4.8	?	?	1.59	?	14.5	10.5
Trunk width, cm (holotype)	1 (1.4 in hepatic region)	0.51 (anterior); 0.22 (posterior)	?	1.3	?	?	damaged	?	0.7	1.5 (anterior); 0.4 (posterior)
	About 100	9	More than 20	About 24	30	About 30	10			About 50 and more

(*continued on next page*)

ARTICLE IN PRESS

Table 2 (*continued*)

	Allapasus aurantiacus	*Allapasus fuscus*	*Allapasus isidis*	*Coleodesmium karaensis*	*Tergivelum baldwinae*	*Tergivelum cinnabarinum*	*Terminstomo arcticus*	*Torquarator bullocki*	*Yoda purpurata*	*Quatuoralisia malakhovi*
Number of pairs of gill pores								About 40 and more	About 40 and more	
Lateral (genital) wings	Yes	Yes	Yes	Yes	Back veils	Back veils	Ridges	Yes	Yes	Yes
Perihaemal coelom	Yes	Yes	Yes	Yes	Yes	Yes	Yes	Yes	No	Yes
Sex	Separated	Separated	Separated	Separated	Separated	Separated	Separated	Separated	Hermaphrodites	Separated
Holotype sex	♀	♀	♂	♀	♂	♂	♀	♀	Hermaphrodite	♂
Paratype sex	♀	No specimens	No specimens	No specimens	♀, ♂	♀, ♂	No specimens	No specimens	Hermaphrodite	♀, ♂
'Externalized' testes	?	?	No	?	No	No	?	?	No	Yes
Externalized ovaries	Yes	Yes	Most likely yes	No	No	No	No	?	No	Yes
Maximum oocyte diameter, μm	1500	950	?	About 1000	1500	400	200	500	300	600
External brooding	?	?	?	Yes	?	?	?	?	?	?
Faecal trail	?	?	?	?	Spiral or meandering	Spiral	?	?	Irregularly meandering	Mainly meandering
Additional distinctive characters	–	Typhlosole process in the collar	No detectable lumen in the buccal diverticulum	Proboscis skeleton has a tubular component ensheathing the collar that has transverse opaque stripe	Laterodorsal fossa in the proboscis; dorsal protuberances in addition to the back veils; paired buccal muscles	Dorsal protuberances in addition to the back veils; paired buccal muscles	Buccal diverticulum terminates in posterior proboscis; deep ventral groove in posterior intestinal region of trunk	Anterior and posterior horns of the proboscis skeleton	Lacks hepatic sacs; nuchal protuberances of collar	Lateral wings are divided into a genital and hepatic regions; two hepatic blood vessels

Fig. 1. Deep-sea enteropneust species from the Bering Sea. (**A**) Aggregation of *Quatuoralisia malakhovi* n. gen. n. sp. on soft substrate, the northern slope of the Volcanologists Massif, 1830–2290 m. (**B**) *Q. malakhovi* n. gen. n. sp. (black arrow) on hard substrate, the northern slope of the Volcanologists Massif, 1830–2290 m. (**C**) Torquaratoridae gen. sp. 1, the northern slope of the Volcanologists Massif, 3450–4278 m. (**D**) Crawling out of a burrow *Saxipendium* sp. (Harrimaniidae), the southern slope of the Volcanologists Massif, 1930 m. (**E**) Harrimaniidae gen. sp. 1, Koryak slope, 660 m. (**F, G**) Harrimaniidae gen. sp. 2 drifting in the near-bottom current (**F**) and buried in sediment (black arrow) (**G**), Koryak slope, 419–420 m. All scale bars are 10 cm.

comparative analysis of all described torquaratorid species is provided. To verify the status of the new genus and species, we conducted molecular analysis based on the mitochondrial 16S rRNA. Additionally, a map is provided with records of all known torquaratorid species, described and undescribed. Data on biology and abundance are discussed.

2. Material and methods

2.1. Sampling and first processing

Enteropneusts of the five species (Table 3) discovered on cruises of the RV *Akademik M.A. Lavrentyev* 75 (2016), 82 (2018), and 93 (2021) were photographed and videotaped *in situ* using the ROV *Comanche 18* equipped with *Canon PowerShot G5* and *Kongsberg Underwater HDTV* colour camera *OE14-502*.

Specimens of one torquaratorid species were sampled on the slope of the Volcanologists Massif (Fig. 2) using a manipulator of the ROV *Comanche 18* in 2016 and a slurp-gun in 2018. Details of the collection sites and material are in Table 4 and Table 5. The freshly collected specimens were photographed using camera *Nikon D800* with a macro lens *Micro Nikkor 60* and the off-camera flash *Nikon SB600*. Photographs of preserved material were taken using camera *Nikon D350*.

For histological studies, the animals were preserved in 8% formaldehyde or 4% paraformaldehyde buffered with seawater; material was stored in fixative for a year in a fridge at –4°C before further processing. For molecular studies, fragments of animals were preserved in 96% ethanol and were kept in a freezer at −20°C.

2.2. Morphological study

The external morphology was studied at the Student Laboratory of Evolutionary Morphology of Animals (www.evolmorphan.ru), Department of Invertebrate Zoology, Biological Faculty of Lomonosov Moscow State University (MSU) using the stereomicroscope *MSP-2 var.2* (LOMO, Saint-Petersburg, Russia, 2018) with a digital camera *MC-12* and the stereomicroscope *Leica M165C* with camera *Leica DFC490* (Leica Biosystems, Germany) in IORAN.

Prior to histological processing, the selected specimens were transferred from a fixative to 70% ethanol and cut into short portions (anterior part of the proboscis, posterior part of the proboscis + collar + anterior part of the trunk, branchiogenital region of the trunk, lateral wing, hepatic and intestinal regions of the trunk) for better impregnation. The samples were then dehydrated through increasing series of ethanol and butanol, embedded in paraplast and sectioned into sections 7 μm and 10 μm thick using a rotational microtome *Leica RM 2125RTS* (Leica Biosystems, Germany). The sections were stained with hematoxylin following standard procedures (Valovaya and Kavtaradze, 1993). In total, seven series were studied using light microscopy (three specimens collected in 2016 and four specimens collected in 2018) (Table 5). Photographs of histological sections were made using the *Micmed-6* microscope (LOMO, Saint-Petersburg, Russia, 2018) with digital camera *MC-12*.

Table 3
Deep-sea enteropneusts from the Bering Sea.

Species	Cruise, station	Material	Locality	References
Torquaratoridae, *Quatuoralisia malakhovi* n. gen. n. sp.	Lavrentyev-75 (st. 17, 18), Lavrentyev-82 (st. 9)	Collected; imaged	Northern slope of the Volcanologists Massif, 1370–2470 m; southern slope of the Volcanologists Massif, 1511–1992 m	Galkin, Ivin, 2019; Vinogradov, 2019; Rybakova et al., 2020; Lukinykh et al., 2018; Ezhova et al., 2021; this paper
Torquaratoridae gen. sp. 1	Lavrentyev-75 (st. 16, 22), Lavrentyev-82 (st. 5)	Not collected; imaged	Komandorsky Graben (55.5774N; 167.3258E), 4278 m; northern slope of the Volcanologists Massif (55.5143N; 167.3272E - 55.5039N; 167.3195E), 3450–3610 m; southern slope of the Volcanologists Massif (55.2763N; 167.2960E - 55.2616N; 167.3025E), 3334–3931 m	Rybakova et al., 2020:9 (as Enteropneusta gen. sp.1); this paper
Harrimaniidae, *Saxipendium* sp.	Lavrentyev-82 (st. 6, 9)	Not collected; imaged	Slope of the basement block to the north-west of the Volcanologists Massif (55.6825N; 167.1075E - 55.6973N; 167.1262E), 3391–3906 m; southern slope of the Volcanologists Massif (55.3471N; 167.2742E), 1930 m	This paper
Harrimaniidae gen. sp. 1	Lavrentyev-82 (st. 14, 18, 21)	Not collected; imaged	Koryak slope (60.8343–61.1195N; 174.3722-174.9650E), 659–662 m	This paper
Harrimaniidae gen. sp. 2	Lavrentyev-93 (st. 5, 6)	Not collected; imaged	Koryak slope (61.1734N; 174.8767E), 419–420 m	This paper

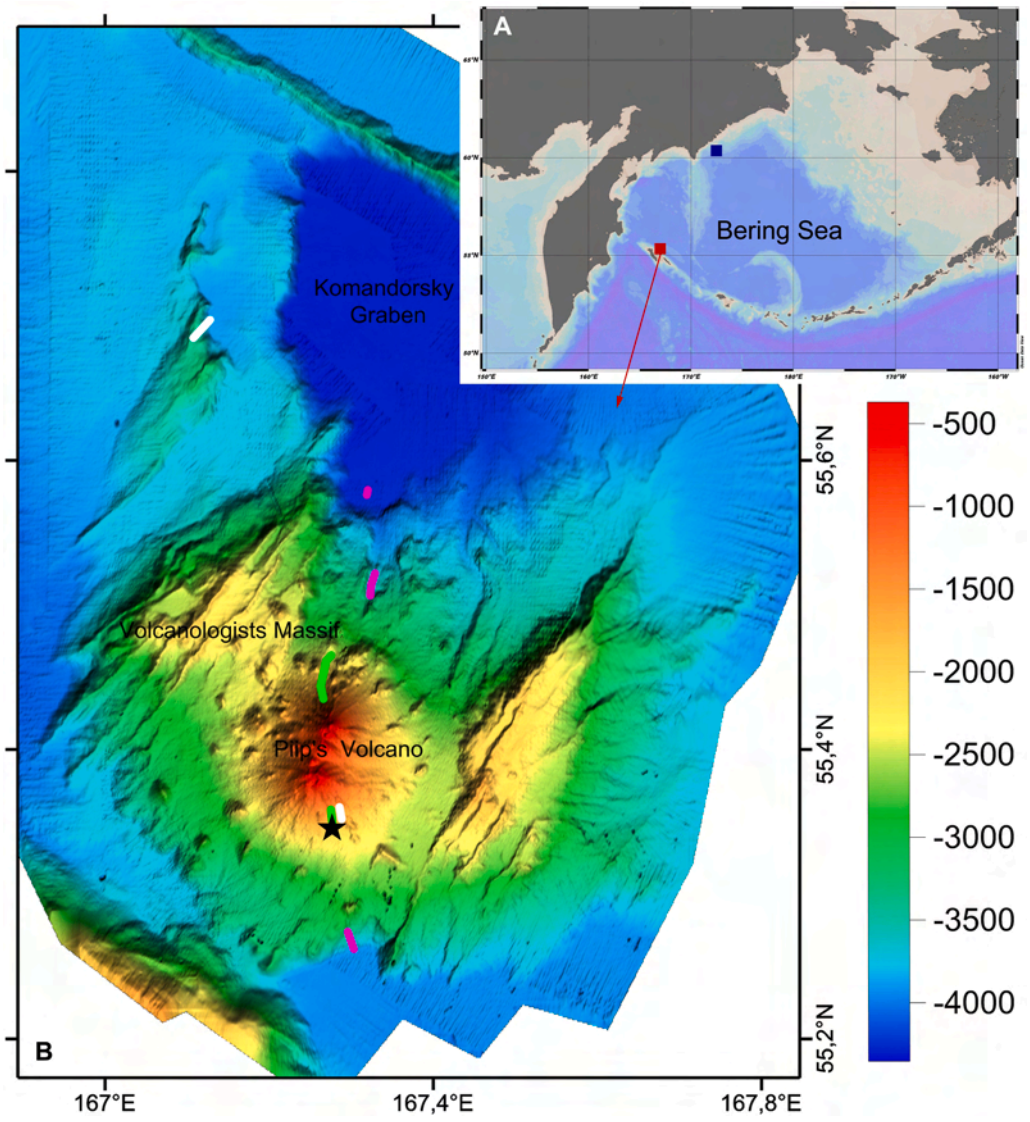

Fig. 2. **A**: Study areas in the Bering Sea: Deep blue square – Koryak slope, finding locality of Harrimaniidae gen. sp. 1 and Harrimaniidae gen. sp. 2. Dark red square – Volcanologistst Massif, Piip Volcano and Komandorsky Graben, finding locality of three species (details in **B**). **B**: Records and collection sites of: *Quatuoralisia malakhovi* n. gen. n. sp. (green) and the type locality (black star); Torquaratoridae gen. sp. 1. (magenta); Harrimaniidae, *Saxipendium* sp. (white).

Table 4
Sampling locations of examined specimens of *Quatuoralisia malakhovi* n. gen. n. sp.

Cruise	Station no.	Date of collection	Coordinates	Depth, m	Number of specimens studied
RV *Akademik M.A. Lavrentyev*, cruise 75	LV 75-17	June 27, 2016	55.4609N 167.2688E	2289	3
RV *Akademik M.A. Lavrentyev*, cruise 82	LV 82-9	June 18, 2018	55.3451-55.3466N 167.2750-167.2752E	1957–1933	8

The frontal series of histological sections of the specimen no. 7 (Table 5) was used for 3D-reconstruction of the two plates of proboscis skeleton. The reconstruction was carried out using the AMIRA software, version 6.5.0. In total, 63 slides were used for reconstruction.

The segments of the branchiogenital region of the trunk including the gill apparatus, lateral wings and gonads were studied using a scanning electron microscope (SEM) (Table 5). The samples for SEM were dehydrated through the acetone following standard procedures (Biserova, 2013), critical-point dried using CO_2 (*HCP-2 Critical Point Dryer*, Hitachi, 1980), sputter-coated with a gold-palladium mixture (*EIKO IB-3 Ion Coater*, 1980) and examined using SEM *JSM*-6380LA (JEOL, 2005) and *Camscan-S2* (Cambridge Instruments, 1990) in the *Electron Microscopy in Life Sciences* Center for Collective Use, MSU.

The studied material is deposited in the collection of the Student Laboratory of Evolutionary Morphology of Animals (www.evolmorphan.ru), Department of Invertebrate Zoology, MSU. The holotype is stored in the Museum of the Institute of Marine Biology, A.V. Zhirmunsky National Scientific Center of Marine Biology, Far Eastern Branch, Russian Academy of Sciences (MIMB), Vladivostok (Russia) (Table 5).

2.3. DNA extraction, amplification, and sequencing

Genomic DNA was extracted from the 50 mg pieces of tissue fixed in

Table 5
Material studied and methods used.

Specimen no.	Station	Status	Preservation	ID (if available)	Collection/ Museum no.	GenBank no.	Sex	Body fragment studied histologically	Section direction	Section thick, μm	Body fragment studied by SEM	Reference to figures
1	LV 75-17	Paratype	8% formaldehyde in sea water	–	2017-QM-01	–	♂	Trunk	Transverse	7	–	Lukinykh et al., 2018
2	LV 75-17	Paratype	8% formaldehyde in sea water	–	2017-QM-02	–	♀	Entire body	Sagittal	7	–	Lukinykh et al., 2018
3	LV 75-17	Paratype	8% formaldehyde in sea water	–	2018-QM-03	–	♂	Branchio-genital region	Transverse	7	Lateral wings (genital region)	–
4[a]	LV 82-9	Paratype	96° ethanol	1 (1375)	AML-82_1 AML-82_21 AML-82_22	MT773355 MT773356 MT773357	♂	–	–	–	–	This paper, 3
5[a]	LV 82-9	Paratype	96° ethanol	3 (1377)	AML-82_31 AML-82_32	MT773358 MT773359	♀	–	–	–	Lateral wings (genital region)	This paper, 3
6	LV 82-9	Paratype	8% formaldehyde in sea water	6 (1380)	2019-QM-04	–	♀	Proboscis, collar, branchio-genital region	Transverse	7	–	This paper, 9; 10A-C
7	LV 82-9	Paratype	8% formaldehyde in sea water	4 (1378)	2020-QM-05	–	♂	Proboscis, collar Genital & hepatic regions Genital wings, intestinal region	Frontal Sagittal Transverse	10	Lateral wings (genital region), sperm	This paper, 4B-D; 6D-F,H,I; 7; 8; 10D-F; 11
8	LV 82-9	Paratype	8% formaldehyde in sea water	5 (1379)	–	–	?	–	–	–	–	–
9	LV 82-9	Paratype	8% formaldehyde in sea water	(1383)	2020-QM-06	–	♀	Proboscis, collar, genital & hepatic regions	Sagittal	10	–	This paper, 5; 6A-C
10	LV 82-9	Paratype	8% formaldehyde in sea water	(1381)	2021-QM-07	–	♀	Proboscis, collar, branchio-genital region	Transverse	7	–	This paper, 6G
11	LV 82-9	***Holotype***	8% formaldehyde in sea water	2 (1376)	MIMB 41549	–	♂	–	–	–	–	–

[a] Specimens for 16S rDNA sequence.

96% ethanol of two specimens, no. 4 and 5 (Table 5) using the *DNeasy Blood & Tissue Kits* according to the protocol of manufacturer (Qiagen Inc., Valencia, CA). PCR amplifications were carried out in a 20-μL reaction volume, which included 4 μL of 5x *Screen Mix-HS* (ready-to-use PCR mixture, Evrogen Lab, Russia), 0.5 μL of each primer (10 μM stock), 1 μL of genomic DNA, and 14 μL of deionized distilled water. Extracted DNA was used as a template for an amplification of mitochondrial 16S rRNA (16S). For amplification and sequencing the following 16S primers were used: 16Sarl (5'-CGCCTGTTTAACAAAAACAT-3') and 16Sbrh (5'-CCGGTCTGAACTCAGATCACGT-3') (Palumbi, 1996). The amplification began with an initial denaturation for 5 min at 95°C, followed by 35 cycles of 15 s at 94°C (denaturation), 45 s at 50°C (annealing temperature), and 60 s at 72°C, with a final extension of 7 min at 72°C. PCR products were sequenced using same primers and *BigDye Terminator v.3.1. Kit* (Applied Biosystems) on *ABI3500* genetic analyzer at Evrogen Lab, Russia.

2.4. Phylogenetic analysis

Row reads were assembled using *Geneious 8.0.5* (Biomatters, Auckland, New Zealand). Original 16S data and publicly available sequences for other species from GenBank (Table 6) were aligned with *MuSCLE* algorithm (Edgar, 2004) in *MEGA7* (Kumar et al., 2016). Final 16S alignment comprised 629 bp.

The best-fitting model for the dataset was the General Time Reversible with gamma distribution (GTR + G), tested using the *MEGA X* (Kumar et al., 2016). The phylogenetic reconstruction was conducted by Maximum Likelihood method implemented in *MEGA X* (Kumar et al., 2016) with 1000 bootstrap pseudoreplications. Bayesian estimation of posterior probability was performed in *MrBayes 3.2* (Ronquist et al., 2012). 50 million Markov chain Monte Carlo (MCMC) steps was used for the analysis. Genetic distances (p-distance) were calculated in the *MEGA X* (Table 7). Final phylogenetic tree images (Fig. 3) were rendered in *Fig Tree Drawing Tool 1.4.3*.

3. Results

3.1. Systematics

Phylum Hemichordata Bateson 1885

Table 6
Specimen and sequence identification in GenBank (NCBI) for taxa used for phylogenetic tree.

Species	16S	Citation
Torquaratoridae		
Allapasus aurantiacus (T438)	JN886748	Osborn et al., 2012
Allapasus aurantiacus (D98-pc66)	JN886750	Osborn et al., 2012
Allapasus isidis (I174-43b)	JN886749	Osborn et al., 2012
Coleodesmium karaensis	KC907711	Osborn et al., 2013
Tergivelum baldwinae (T1094)	EU520497	Holland et al., 2009
Tergivelum baldwinae (T10762)	EU520496	Holland et al., 2009
Tergivelum baldwinae (T10761)	EU520494	Holland et al., 2009
Tergivelum baldwinae (T10781)	EU520495	Holland et al., 2009; Osborn et al., 2012
Tergivelum cinnabarinum (I163-17)	JN886752	Osborn et al., 2012
Tergivelum cinnabarinum (I165-24)	JN886753	Osborn et al., 2012
Tergivelum cinnabarinum (I168-28)	JN886754	Osborn et al., 2012
Yoda purpurata (I171-36a)	JN886740	Osborn et al., 2012
Yoda purpurata (I171-36b)	JN886741	Osborn et al., 2012
Yoda purpurata (I174-43a)	JN886742	Osborn et al., 2012
Genus B sp. 1 (T879-A8)	EU520500	Holland et al., 2009; Osborn et al., 2012
Genus B sp. 1 (T879-A10)	EU520501	Holland et al., 2009
Genus B sp. 1 (T879-A8)	JN886743	Osborn et al., 2012
Genus B sp. 1 (D176-A1)	JN886744	Osborn et al., 2012
Genus B sp. 1 (D176-A5)	JN886745	Osborn et al., 2012
Genus B sp. 1 (D176-A2)	JN886746	Osborn et al., 2012
Genus B sp. 2 (T1013-A8)	EU520502	Holland et al., 2009
Genus B sp. 2 (T1011)	EU520503	Holland et al., 2009
Genus B sp. 2 (D177-A28)	JN886747	Osborn et al., 2012
Genus C sp. 1 (T886-A4)	EU520499	Holland et al., 2009
Genus C sp. 1 (T1012-A8)	EU520498	Holland et al., 2009
Genus C sp. 1 (D80-A2)	JN886751	Osborn et al., 2012
Torquaratoridae sp. (H90.3)	KF683552	Halanych et al., 2013
Torquaratoridae sp. (H78-1)	KF683553	Cannon et al., 2013
***Quatuoralisia malakhovi* n. gen. n. sp. (AML-82_21)**	**MT773356**	This study
***Quatuoralisia malakhovi* n. gen. n. sp. (AML-82_31)**	**MT773358**	This study
Ptychoderidae		
Balanoglossus carnosus	LC120744	Urata, 2016
Balanoglossus carnosus	LC120754	Urata, 2016
Balanoglossus clavigerus	EU728425	Cannon et al., 2009
Glossobalanus berkeleyi	EU728426	Cannon et al., 2009
Glossobalanus berkeleyi (H68.2)	KF683554	Cannon et al., 2013
Ptychodera flava	LC018637	Urata, 2015
Ptychodera flava	EU728428	Cannon et al., 2009
Ptychodera flava	EU728429	Cannon et al., 2009
Ptychodera bahamensis (H54.1)	KF683560	Cannon et al., 2013
Ptychoderidae sp. WCJ2000	EU728427	Cannon et al., 2009
Spengelidae		
Glandiceps hacksi	JN886755	Osborn et al., 2012
Glandiceps abyssicola	KC776732	Holland et al., 2013
Schizocardium brasiliense	NC_040108	Li et al., 2019
Harrimaniidae		
Saccoglossus mereschkowskii (H53.1)	KF683545	Cannon et al., 2013
Saccoglossus pusillus	EU728422	Cannon et al., 2009
Harrimania planktophilus	EU728421	Cannon et al., 2009
Protoglossus koehleri	EU728420	Cannon et al., 2009
Saxipendium coronatum	EU728423	Cannon et al., 2009
Saxipendium coronatum	EU520493	Holland et al., 2009
Saxipendium sp. 1 (D176-A11)	JN886756	Osborn et al., 2012
Echinodermata		
Asterias forbesi	DQ297073	Janies, 2006
Aspidodiadema jacobyi	DQ073734	Smith et al., 2006

Class Enteropneusta Gegenbaur 1870

Family Torquaratoridae Holland, Clague, Gordon, Gebruk, Pawson et Vecchione, 2005.

Torquaratoridae – Holland et al., 2005: 374.

Torquaratoridae – Osborn et al., 2012: 1649 (diagnosis amended); Jabr et al., 2018: 1222.

Diagnosis: Enteropneusts up to 28 cm, with semitransparent, often colored three-part body consisting of broad, short, dome-shaped proboscis, wide collar, and trunk. Muscular system poorly developed. Y-shaped proboscis skeleton or nuchal skeleton absent or reduced to two small plates; horns of proboscis skeleton absent or reduced. Adult buccal diverticulum absent or separated from buccal cavity. Prominent hepatic caeca present, but synapticles absent. Mesocoel ducts and mesocoel pores found only in *Quatuoralisia* n. gen.

Remarks: We amended the family diagnosis to include the characters of a new genus *Quatuoralisia* n. gen., such as the presence of two plates of proboscis skeleton and presence of mesocoel ducts and mesocoel pores. Earlier in the family only one plate in the proboscis skeleton was known and mesocoel ducts and mesocoel pores have not been reported.

The collar in some species is extended laterally forming the so-called lateral lips (Table 2). In most torquaratorids, two sheet-like folds (the lateral or genital wings, the back veils) stretch along the lateral sides of the trunk in the anteroposterior direction. The lateral wings arch over the dorsal surface forming the peribranchial cavity (Holland et al., 2005, 2009; Priede et al., 2012). Musculature is poorly developed as a result of epibenthic or bentho-pelagic life (Holland et al., 2009, 2012a; Priede et al., 2012; Osborn et al., 2013). Only in *Allapasus*, the muscles are significantly developed due to ability to burrow into the surface layer of sediment (Holland et al., 2012a; Priede et al., 2012). The collagen Y-shaped proboscis skeleton is reduced or absent. The gill skeletal bars are delicate, and they are not joined by synapticles. Most of Torquaratoridae have separate sexes except of *Yoda purpurata*, which is the only known hermaphrodite among the phylum Hemichordata (Priede et al., 2012). Species of *Allapasus* (Table 2) are characterized by so-called externalized ovaries, extruding into the peribranchial cavity and surrounded by a thin jelly layer and germinal epithelium (Holland et al., 2012a; Jabr et al., 2018). For *Coleodesmium karaensis*, the "external brooding" of embryos into the epithelium of female genital wing has even been described (Holland et al., 2012a; Osborn et al., 2013; Jabr et al., 2018).

Species of all seven genera currently included in this family – *Allapasus*, *Coleodesmium*, *Tergivelum*, *Terminstomo*, *Torquarator*, *Yoda* and *Quatuoralisia* n. gen. are found exclusively in the deep sea.

Genus *Quatuoralisia* new genus Ezhova et Lukinykh.

Type species: *Quatuoralisia malakhovi* n. gen. n. sp. described herein.

Etymology: Referring to unique morphological feature of described enteropneusts: separation of each lateral wing into two regions, resulting in the presence of four "wings" ("*quatuor alis*"); gender feminine.

Diagnosis: Each lateral wing with constriction dividing it into anterior genital region and posterior hepatic region. Y-shaped proboscis skeleton represented by two plates. Heart-kidney complex comprises pericardial coelomic sac, glomerulus filled with tiny coelomic tubules, and buccal diverticulum. Buccal cavity absent. Collar has two symmetric mesocoel ducts and mesocoel pores. Testes bulging into peribranchial cavity above genital region surface of lateral wings.

Included species: Only the type species.

Distribution: south-western Bering Sea, slopes of the Volcanologists Massif, 1370–2470 m.

Differences from similar genera: External morphology is somewhat similar to "Genus C" (see Osborn et al., 2012, Fig.1J) and to *Torquarator bullocki* (Holland et al., 2005, Fig. 1). However, according to N. Holland's personal communication (April 21, 2019), the lateral wings of *T. bullocki* lack the constriction between the anterior and posterior regions of the wing. Detailed morphological data of "Genus C" were not published, however it was mentioned as narrow-lipped torquaratorid (Osborn et al., 2012), thus the collar of "Genus C" lacks conspicuous lateral lips.

***Quatuoralisia malakhovi* new species Ezhova et Lukinykh.**

(Fig. 1A and B, 4–12)

Species nova – Vinogradov, 2019.

Torquaratoridae gen. sp. – Rybakova et al., 2020; Lukinykh et al., 2018; Ezhova et al., 2021.

Etymology: Species name is in honor of our tutor, Professor Vladimir V. Malakhov.

Table 7
Intraspecies and interspecies p-distances between Torquaratoridae species calculated for 16S marker.

No.	Species	1	2	3	4	5	6	7	8	9	10	11	12	13	14
1	*Quatuoralisia malakhovi* n. gen. n. sp.	0,0000													
2	*Quatuoralisia malakhovi* n. gen. n. sp.	0,0452	0,0452												
3	Genus C	0,0379	0,0379	0,0397											
4	Torquaratoridae sp. H90-3	0,0617	0,0617	0,0600	0,0472										
5	*Coleodesmium karaensis*	0,0625	0,0625	0,0608	0,0478	0,0000						0,0018			
6	Torquaratoridae sp. H78-1	0,0922	0,0922	0,0870	0,0759	0,0782	0,0792					0,0038	0,0019		
7	*Tergivelum baldwinae*	0,0904	0,0904	0,0906	0,0723	0,0727	0,0737	0,0108				0,0096	0,0126	0,0113	
8	*Tergivelum cinnabarinum*	0,0793	0,0793	0,0668	0,0631	0,0726	0,0735	0,0759	0,0741			0,0144	0,0485	0,0488	0,0503
9	*Allapasus aurantiacus*	0,0812	0,0812	0,0634	0,0597	0,0745	0,0755	0,0743	0,0743	0,0217					
10	*Allapasus isidis*	0,1119	0,1119	0,1157	0,1083	0,1143	0,1158	0,1209	0,1173	0,1029	0,1103				
11	Genus B sp. 1 T879-A8	0,1101	0,1101	0,1139	0,1065	0,1125	0,1140	0,1191	0,1155	0,1011	0,1085	0,0503			
12	Genus B sp. 1 T879-A10	0,1113	0,1113	0,1153	0,1075	0,1139	0,1139	0,1208	0,1170	0,1019	0,1096	0,1067	0,0993		
13	Genus B sp. 1 D176-A2	0,1119	0,1119	0,1175	0,1029	0,1107	0,1121	0,1155	0,1101	0,0993	0,1067	0,1139	0,1081	0,1191	
14	Genus B sp. 2 T1013-A8	0,1137	0,1137	0,1245	0,1117	0,1234	0,1250	0,1245	0,1191	0,1081	0,1139	0,1139	0,1081	0,1191	0,1245
15	*Yoda purpurata*	0,1137	0,1137	0,1245	0,1117	0,1234	0,1250	0,1245	0,1191	0,1081	0,1139	0,1139	0,1081	0,1191	0,1245

Type material: MIMB 41549: holotype, complete spm., male; RV *Akademik M.A. Lavrentyev*, cruise 82, st. 9, 55.3451-55.3466N, 167.2750-167.2752E, June 18, 2018, ROV *Comanche 18*, 1957–1933 m, slurp-gun, preserved in formalin. Student Laboratory of Evolutionary Morphology of Animals (www.evolmorphan.ru) of the Department of Invertebrate Zoology, MSU: paratypes, 9 spms, some of which sectioned (Table 5); the same station as for holotype.

Material examined: Type material.

Type locality: south-west Bering Sea, Volcanologists Massif, 55.3451-55.3466N, 167.2750-167.2752E, 1957–1933 m (RV *Akademik M.A. Lavrentyev*, st. 9).

Diagnosis: A species of *Quatuoralisia* with length reaching 17 cm, with low dome proboscis bearing several short grooves on ventral, dorsal and lateral sides. Slender proboscis stalk absent; proboscis adjoins widely to collar on dorsal side. Developed pericardium; no heart; no proboscis duct. Buccal diverticulum without lumen, separated from pharyngeal wall by basal lamina. Collar has additional midventral lip. Gill pores about 50 pairs and more. Two hepatic blood vessels located ventrally from hepatic sacculations.

Distribution: south-western Bering Sea, slopes of the Volcanologists Massif, 1830–2289 m.

3.2. Description

3.2.1. External anatomy

Large animals reaching 17 cm in length (Table 2; Fig. 4A–C). In nature, semitransparent. Proboscis, collar, and intestinal part of trunk colorless (Fig. 4A). Gonads white, light yellow, cream, or light brown. Hepatic region light blue. In intestinal region, ingested sediment visible through translucent epithelium and intestinal wall (Fig. 4A). Dorsal blood vessel (Fig. 4A, *dbv*), and dorsal nerve cord (Fig. 4B, D, *dn*) may be visible along dorsal midline. Anus is terminal, on the posterior end of the body (Fig. 4A, *an*). Proboscis, collar, and branchiogenital region of freshly collected specimens are tan; hepatic and intestinal regions light yellow with pale blue shade; on entire lateral wings slight "marble" striation (Fig. 4B and C).

Proboscis short, dome-like, with several short longitudinal grooves more or less evenly distributed on lateral, ventral and dorsal sides in proximal area (Fig. 4 A–C). In some specimens, two symmetric parallel dorsal grooves are visible (Fig. 4B, arrowheads). Collar crown-shaped with two wide lateral lips clearly protrude on the sides of the collar (Fig. 4B–D, *llp*, *rlp*), with unpaired medial lip on ventral side, behind the mouth (Fig. 4C, *mlp*). Collar has distinct posterior transverse crest (Fig. 4, *cc*), and has no middorsal groove (Fig. 4A). Midventral collar lip retracted into the mouth in some collected specimens forming collar midventral groove. Mouth leads directly into respiratory pharynx, gill bars visible in open mouth.

Trunk subdivided into three regions: branchiogenital with gill pores and gonads, hepatic with hepatic sacculations, and intestinal (Fig. 4A and B). Branchiogenital and hepatic regions bear two wide lateral wings. Each wing subdivided by transverse constriction into anterior genital region (Fig. 4, *bgw*) and posterior hepatic region (Fig. 4, *hpw*). Lateral wings arch over dorsal surface forming peribranchial cavity. Edges of wings meet along dorsal midline, cover the middorsal ridge (Fig. 4D, *mdr*), but do not fuse (Fig. 4A, B, D); sometimes wings gape apart from each other, especially in hepatic region (Fig. 4A). Middorsal ridge runs along left and right rows of the gill pores in branchiogenital region (Fig. 4D, *gp*), and left and right rows of greenish-brown hepatic sacculations in hepatic region (Fig. 4D, *hs*). Number of pairs of gill pores can reach 50 or more. Number of hepatic sacculations near 30 in each row. Numerous gonads located on surface of genital region of wings that faces to peribranchial cavity (Fig. 4D, *gon*). Gonads protrude into peribranchial cavity and look similar in males and females, however testes larger that ovaries. Dorsal nerve cord visible within middorsal ridge and above translucent intestine (Fig. 4B, D, *dn*). On ventral side of trunk, midventral groove runs between bases of lateral wings (Fig. 4C, *mvg*).

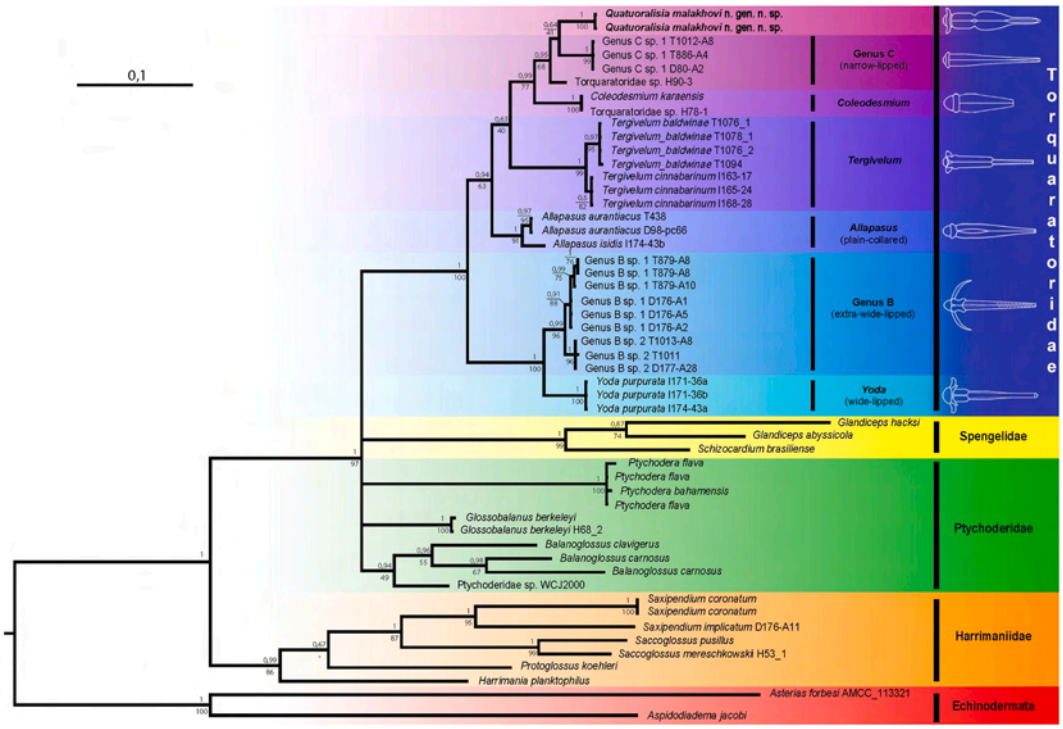

Fig. 3. Phylogenetic reconstruction of Enteropneusta based on 16S rDNA. Numbers above nodes indicate posterior probability and numbers under nodes indicate bootstraps from the maximum likelihood analysis. Images of torquaratorids are not to scale.

Midventral trunk groove accompanied by ventral nerve cord (Fig. 4C, *vn*).

See measurements in Table 2.

3.2.2. *Internal anatomy*

Ectoderm epithelium approximately 100–500 μm high, and consists of columnar cells (mainly in proboscis and collar) and numerous light vacuolated glandular cells (Figs. 5, 6A, 7, 8B, 9, 10A, B and 11). General intraepidermal nerve plexus poorly developed. It forms several thickenings: 1) two lateral proboscis nerves going along left and right prolongations of proboscis-collar septum (Figs. 7 and 8B, *lpn*), 2) lateral pharyngeal nerves (Figs. 7 and 8A, C, *phn*), 3) collar nerve cord (Figs. 5 and 6G, *cnc*), 4) trunk dorsal nerve cord (Figs. 9, 10A and 11, *dn*) and 5) trunk ventral nerve cord (Figs. 9, 10B and 11, *vn*). Thickened collagen plates, i.e., hypertrophy of basal lamina, underlay these nerves (Figs. 6G, 8A–C and 10A). Triangular collagen plates between lateral proboscis nerves, pharyngeal nerves and buccal diverticulum (Figs. 6H, I, 7 and 8A–C, *sk*) represent two plates of reduced Y-shaped proboscis skeleton.

Generally, muscle cells sparsely scattered in coelomic cavities not obviously oriented in any particular direction (Figs. 5, 6B, 7, 9, 10B and 11). Longitudinal buccal muscles are clear visible in collar (Fig. 8A–C, *bcm*). They attach to proboscis-collar septum, and to skeletal plates of proboscis skeleton, and extend along sides of mouth in anteroposterior direction (Fig. 8A–C). Buccal muscles develop from collar coeloms. In perihaemal coeloms, muscle cells form compact longitudinal bands (Figs. 6G, 8D and 10A, *plm*), which extend to posterior wall of proboscis (Fig. 8D). Small concentration of longitudinal muscle fibers presents on ventral side of trunk (Fig. 10B, *mc*).

Heart-kidney complex includes pericardium, and short, but wide glomerulus, lying on wide buccal diverticulum ("stomochord") (Figs. 5, 6A, B, 7 and 8A). Pericardium is small coelomic cavity without ducts (Fig. 6A and B, *pcd*). It adjoins dorsally to buccal diverticulum. The latter consists of light vacuolated cells, and abuts proximal proboscis wall (Figs. 5, 6A, B, 7 and 8A, *bd*). Buccal diverticulum lacks a lumen, and do not connect to pharyngeal roof. Visible septum separates pericardium from perihaemal coeloms (Fig. 6B, arrowheads). Glomerulus is 3-dimensional haemocoelic net of capillaries passing between numerous tiny coelomic tubules (Figs. 6B and 8A, *gl*). It embraces dorsal-anterior side of buccal diverticulum (Fig. 6B). Dorsal blood vessel flows directly into glomerular capillary net (Fig. 8D, *dbv*); distinct heart absent. Proboscis duct not found.

Slender proboscis stalk absent. Instead, proboscis connects widely to collar on dorsal side. Wide proboscis-collar septum consists of two symmetric prolongated halves (Figs. 7 and 8A and B, *pcs*).

Mouth opens ventrally (Fig. 5, *m*). Posterior wall of proboscis represents frontal edge of mouth and collar embraces mouth from sides (Fig. 7). There is no buccal cavity; mouth leads directly into gill pharynx (Fig. 6A).

Two symmetrical mesocoel ducts open into collar coelom to left and right of mid-dorsal line (Fig. 8D, *cld*) via ciliary funnels (Fig. 8E and F, double arrowheads) near first pair of gill bars. Short curved duct tubes pass within collar-trunk septum and continue within epiderm epithelium (Fig. 8D). Their ends protrude freely from epiderm epithelium (Fig. 5, *cld*) and open to exterior also via few pores (Fig. 8E and F, arrowheads).

Branchiogenital region of the trunk contains gill apparatus, and gonads (Figs. 6A, C–F, 9). Gill bars are arranged on each side in two symmetrical rows (Fig. 6D). Primary gill bars ("septa") form more lateral rows (Fig. 6E, *gb-I*) with gill slits between bars (Fig. 6E, *gs*). Secondary gill bars ("tongue bars") form more medial rows, and hang freely into pharyngeal cavity (Fig. 6F, *gb-II*). Synapticles absent. Skeletal elements of gill bars have form of trident with one thick central prong and two thin marginal prongs. Each central prong consists of two fused thin prongs, and supports the primary gill bar (Fig. 6C, *cp*); each secondary gill bar is supported by two marginal prongs of adjacent skeletal tridents (Fig. 6C, *mp*). Each gill bar contains conspicuous coelomic cavity, which represents the peripharyngeal diverticulum of main trunk coelom (Fig. 6C, *tcl*). Gill pharynx is divided into the dorsal respiratory zone (Fig. 9, *ph*), and ventral digestive zone (Fig. 9, *dz*).

Sexes are separate, although it is not easily distinguished without stereomicroscope. Numerous gonads are located in coelom of lateral wings in their genital region (Figs. 4D and 9). Ovaries and testes open

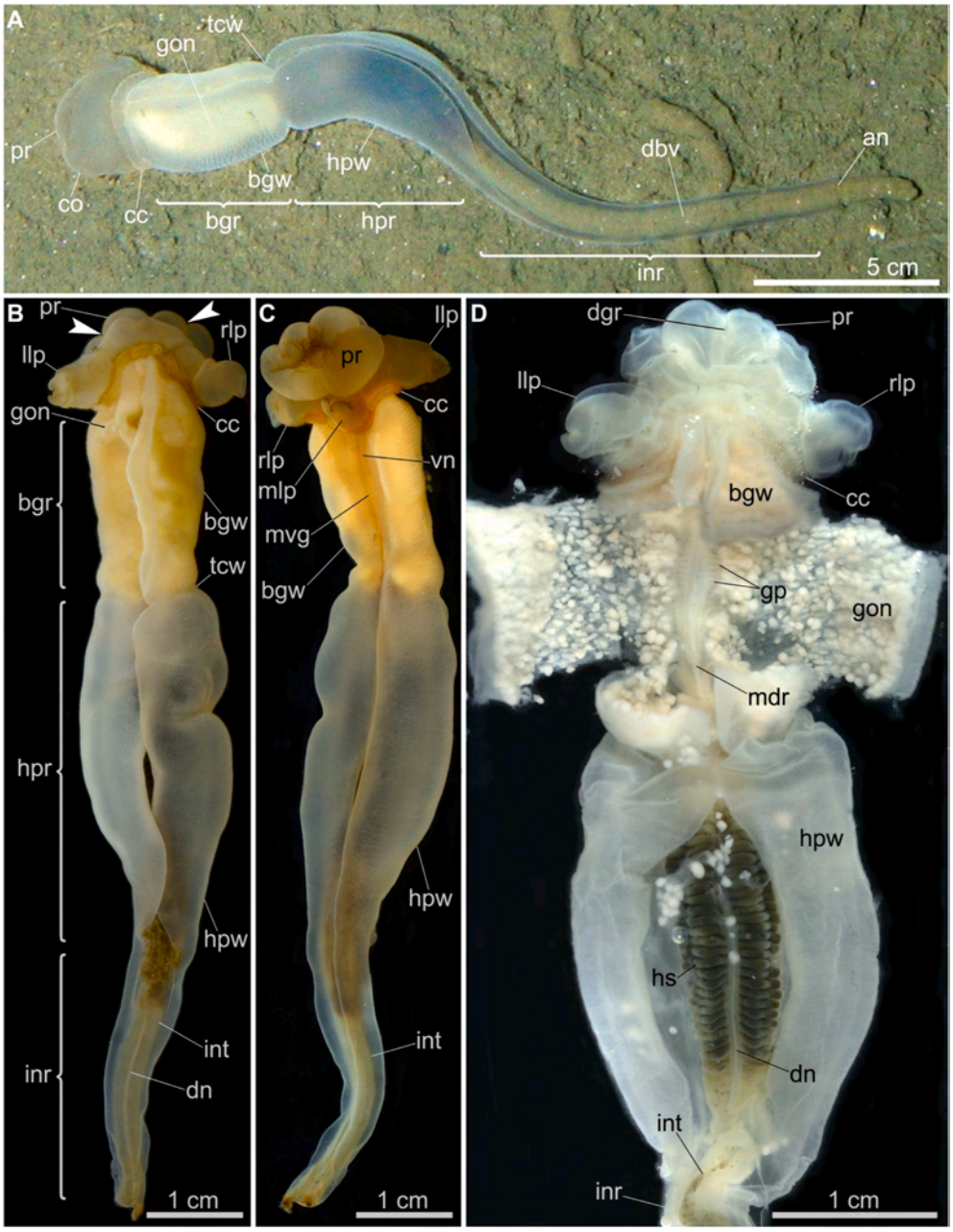

Fig. 4. External features of *Quatuoralisia malakhovi* n. gen. n. sp. **A**: In nature. **B**, **C**: Dorsal and ventral view of a freshly collected specimen no. 7 (Table 5). Arrowheads show the short longitudinal grooves in the proximal area of the proboscis. **D**: The same specimen before cutting with stretched genital regions of wings (*bgw*) and hepatic regions of wings (*hpw*). *an*, anus; *bgr*, branchiogenital region of the trunk; *bgw*, genital region of the lateral wing; *cc*, collar transverse crest; *co*, collar; *dbv*, dorsal blood vessel; *dgr*, dorsal longitudinal groove of the proboscis; *dn*, dorsal nerve cord; *gon*, gonads; *gp*, gill pores; *hpr*, hepatic region of the trunk; *hpw*, hepatic region of the lateral wing; *hs*, hepatic sacculations; *inr*, intestinal region of the trunk; *int*, intestine; *llp*, left collar lip; *mdr*, middorsal ridge; *mlp*, midventral collar lip; *mvg*, midventral groove; *pr*, proboscis; *rlp*, right collar lip; *tcw*, transverse constriction of the lateral wing; *vn*, ventral nerve cord.

into peribranchial cavity via gonopores (one gonopore to one ovary/testis) (Fig. 10C and D, *gnp*). Each ovary contains several oocytes (Fig. 10C, *ooc*) with diameter varying from 50 μm to 600 μm, and yolk cells (Fig. 10C, *yc*). Ripe testes are filled with numerous spermatozoa (Fig. 10D, *sp*). Germinal epithelium comprising spermatogonia, spermatocytes and spermatids is located in peripheric area of testis (Fig. 10D, *ge*).

Hepatic region of trunk bears numerous paired hepatic sacculations along middorsal line (Fig. 4D, *hs*). Hepatic sacculations represent lateral outgrowths of intestinal tube, covered by thin ectoderm epithelium and protrude into cavity under lateral wings (hepatic region of the wings) (Fig. 11A). On ventral side, gastrodermal epithelium of hepatic sacculations is corrugated into dozen plicae on each side of midline (Fig. 11A). Right and left hepatic blood vessels accompany hepatic sacculations here (Figs. 10E and F, *rhv*, *lhv*, 11A). These vessels run through the trunk coelom; in some sections, thin mesenterial connections between hepatic blood vessels and hepatic gastrodermal epithelium are visible (Fig. 10E and F, double arrowheads). Structure of dorsal and ventral mesenteries is the same as in branchiogenital region (Fig. 10A and B).

Intestinal region of trunk contains intestine flanked with left and right narrow cavities of trunk coelom with dorsal and ventral mesenteries between them, where the dorsal and ventral blood vessels continue (Fig. 11B). Hepatic blood vessels are not visible here.

3.3. Molecular analysis

Molecular analysis of the 16S gene revealed that *Quatuoralisia malakhovi* n. gen. n. sp. is clustering with representatives of the family Torquaratoridae (Fig. 3). Two examined specimens of *Q. malakhovi* form a tight cluster. *Q. malakhovi* is genetically most closely related to an undescribed species originally designated as narrow-lipped "Genus C" by Osborn et al. (2012) (a genetic divergence of 4.52%), and to antarctic Torquaratoridae sp. H90-3 (Halanych et al., 2013) (a genetic divergence of 3.79%) (Table 7).

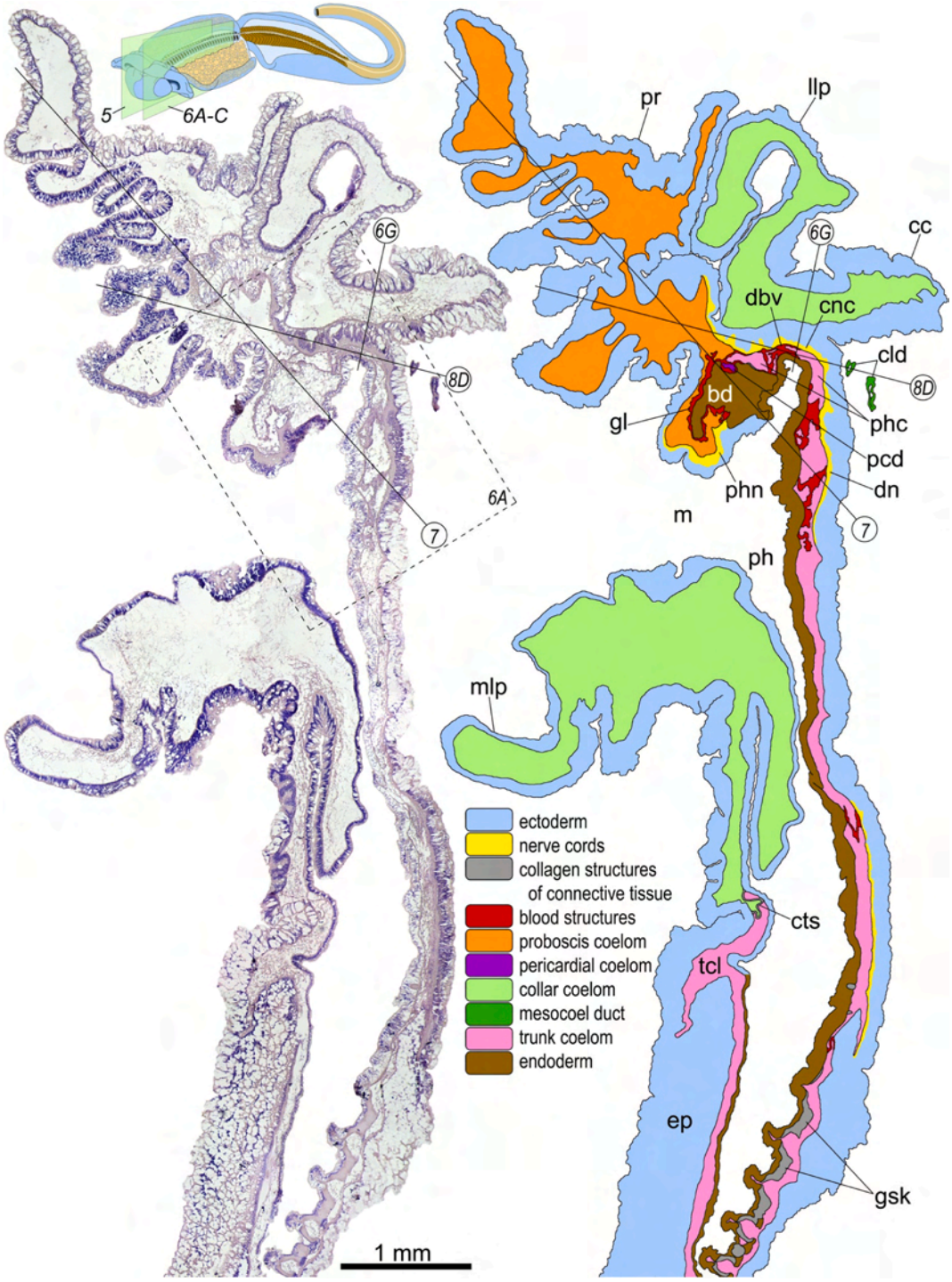

Fig. 5. Proboscis, collar, and anterior part of the trunk of *Quatuoralisia malakhovi* n. gen. n. sp., sagittal section. Lines indicate the level of the transverse section of Fig. 6G, and the frontal section of Figs. 7 and 8D. Dotted rectangle indicates the structures shown in Fig. 6A *bd*, buccal diverticulum; *bgw*, genital region of the lateral wing; *cc*, collar transverse crest; *cld*, mesocoel duct; *cnc*, collar nerve cord; *cts*, collar-trunk septum; *dbv*, dorsal blood vessel; *dn*, dorsal nerve cord; *ep*, ectoderm epithelium; *gl*, glomerulus; *gsk*, gill skeletal elements; *llp*, left collar lip; *m*, mouth; *mlp*, midventral collar lip; *pcd*, pericardium; *ph*, cavity of the pharynx; *phc*, perihaemal coelom; *phn*, lateral pharyngeal nerve; *pr*, proboscis; *tcl*, main trunk coelom.

3.4. Deep-sea enteropneusts of the western Bering Sea inferred from video and photography

In addition to *Quatuoralisia malakhovi* n. gen. n. sp., four other deep-sea enteropneust species were recorded in the western Bering Sea on video (Table 3). One species, Torquaratoridae gen. sp. 1, was observed in the Komandorsky Graben at the depth of 4278 m and on the northern and southern slopes of the Volcanologists Massif at the depths 3334–3931 m (Fig. 2, magenta). It is a large animal reaching 18 cm in length, transparent, with signs of violet colouring and with a short proboscis and well-developed lateral collar lips (Fig. 1C). Lateral wings are of the shape of back veils. Specimens were not collected so the generic identification is not available.

Third species recorded from the Volcanologists Massif was a representative of the family Harrimaniidae. It was observed in approximately 34 km to the north-west from the Piip Volcano at the depths 3391–3906

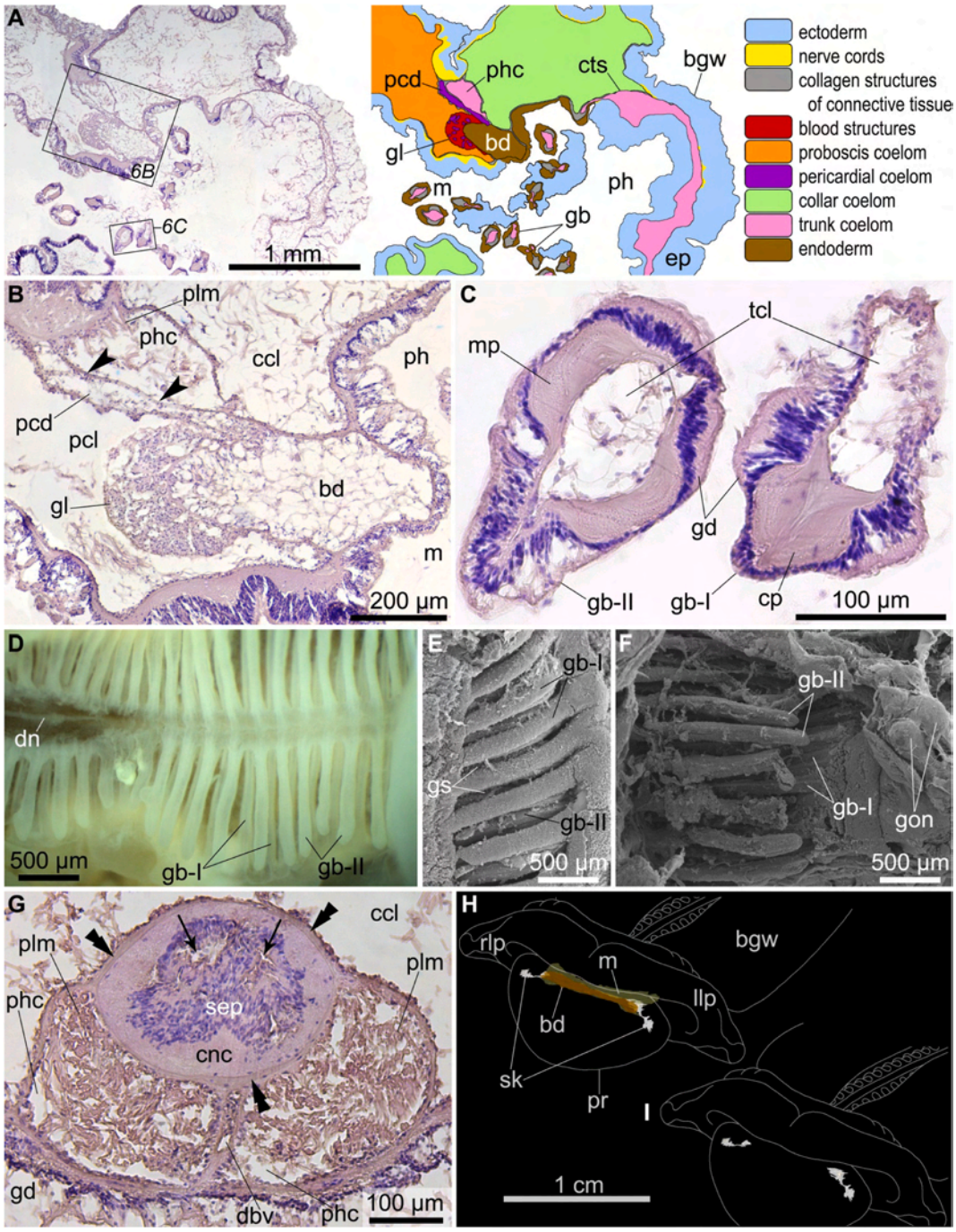

Fig. 6. Histology of proboscis and collar of *Quatuoralisia malakhovi* n. gen. n. sp., parasagittal (**A**–**C**) and transverse (**G**) sections; gill apparatus (**D**–**F**); reconstruction of skeletal plates of proboscis skeleton (**H**, **I**). **A**: Mouth (*m*), and posterior part of the proboscis; the framed rectangle is enlarged in **B**, and **C**. **B**: Heart-kidney complex, i.e., glomerulus (*gl*), pericardium (*pcd*), and buccal diverticulum (*bd*). Arrowheads indicate the septum between the pericardial coelom (*pcd*) and the perihaemal coelom (*phs*). **C**: Transverse section of gill bars. **D**: Dissected branchial pharynx with gill bars. **E**: Gill slits and primary gill bars ("septa") (*gb-I*) (SEM). **F**: Secondary gill bars ("tongue bars") (*gb-II*) (SEM). **G**: Collar nerve cord (*cnc*) on the transverse section. Arrows show the small blind lumens in the cellular part of the collar nerve cord (i.e., in submerged epithelium). Double arrowheads show the thickened collagen plate of connective tissue under the nerve cords. **H**: Location of the skeletal plates (*sk*) relative to the buccal diverticulum (*bd*) and mouth (*m*). **I**: Paired skeletal plates of proboscis skeleton. *bd*, buccal diverticulum; *bgw*, genital region of the lateral wing; *ccl*, collar coelom; *cnc*, collar nerve cord; *cp*, central prong of the gill skeletal element; *cts*, collar-trunk septum; *dbv*, dorsal blood vessel; *dn*, dorsal nerve cord; *ep*, ectoderm epithelium; *gb*, gill bars; *gb-I*, primary gill bars ("septa"); *gb-II*, secondary gill bars ("tongue bars"); *gd*, gastrodermal epithelium; *gl*, glomerulus; *gon*, gonads; *gs*, gill slits; *llp*, left collar lip; *m*, mouth; *mp*, marginal prong of the gill skeleton element; *pcd*, pericardium; *pcl*, proboscis coelom; *ph*, cavity of the pharynx; *phc*, perihaemal coelom; *plm*, perihaemal longitudinal muscles; *pr*, proboscis; *rlp*, right collar lip; *sep*, submerged epithelium of collar nerve cord; *sk*, skeletal plates of proboscis skeleton; *tcl*, peripharyngeal coelomic diverticula of trunk coelom.

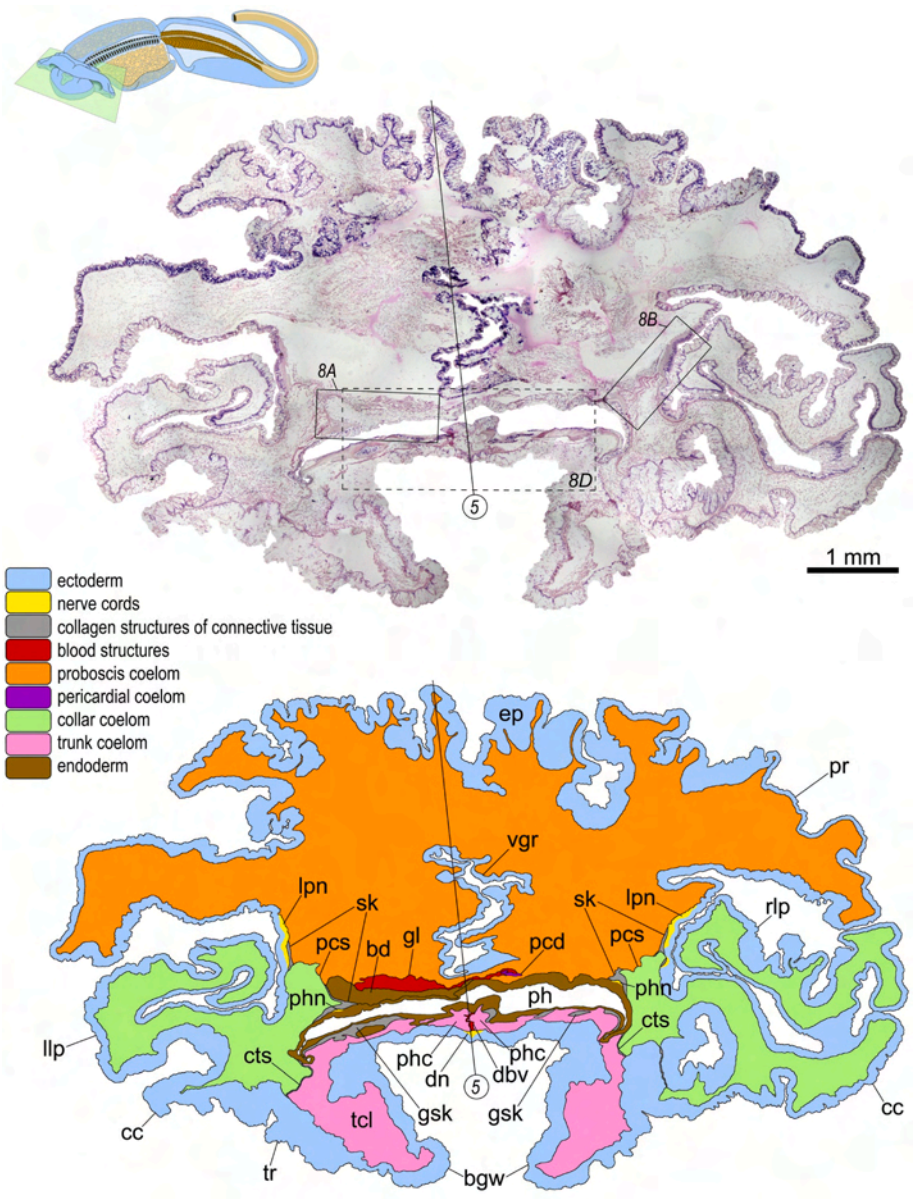

Fig. 7. Proboscis, collar, and anterior part of the trunk of *Quatuoralisia malakhovi* n. gen. n. sp., frontal section. Line indicates the level of the sagittal section of Fig. 5. Frames indicate the structures shown in Fig. 8A and B. Dotted rectangle indicates structures shown in Fig. 8D *bd*, buccal diverticulum; *bgw*, genital region of the lateral wing; *cc*, collar transverse crest; *cts*, collar-trunk septum; *dbv*, dorsal blood vessel; *dn*, dorsal nerve cord; *ep*, ectoderm epithelium; *gl*, glomerulus; *gsk*, gill skeletal elements; *llp*, left collar lip; *lpn*, lateral proboscis nerves; *pcd*, pericardium; *pcs*, proboscis-collar septum; *ph*, cavity of the pharynx; *phc*, perihaemal coelom; *phn*, lateral pharyngeal nerve; *pr*, proboscis; *rlp*, right collar lip; *sk*, skeletal plates of proboscis skeleton; *tcl*, main trunk coelom; *tr*, trunk; *vgr*, ventral longitudinal groove of the proboscis.

m and on the southern slope of the Volcanologists Massif at the depth ~1930 m (Fig. 2, white) together with *Quatuoralisia malakhovi* n. gen. n. sp. It is quite long, about 20 cm, with well-contractile proboscis and narrow collar (Fig. 1D). Proboscis, collar and anterior trunk are of a yellowish colour, the posterior trunk is light violet. Based on visible characters, we tentatively identify it as *Saxipendium* sp. according to the genus and type species diagnosis (Deland et al., 2010). Proboscis is arrow shaped, longer than broad, with the dorsal groove. Collar is short with elevated ring at its posterior end. Trunk is flattened dorsoventrally, with a median longitudinal groove between the rows of gill pores. Dorsolateral genital ridges present on each side of the pharyngeal portion of trunk.

Two more species, tentatively designated as Harrimaniidae gen. sp. 1 and Harrimaniidae gen. sp. 2, were recorded on the Koryak slope at the depth of 659–662 m and 419–420 m correspondingly. In Harrimaniidae gen. sp. 1, proboscis, collar and anterior trunk are of a red colour, the colour of posterior trunk is unknown (Fig. 1E). In Harrimaniidae gen. sp. 2 proboscis and collar are red and trunk is white (Fig. 1F and G).

3.5. Ecology

Quatuoralisia malakhovi n. gen. n. sp. is an epibenthic surface-dweller. During observations, animals were almost motionless or slowly crawling along the seafloor collecting surface deposit using the wide collar lips (Fig. 12A and B). Although *Q. malakhovi* is mainly associated with soft sediments (Figs. 1A and 4A), this species was also found on the hard substrate (Fig. 1B). Based on our observations, this species occurred in habitats with sediment cover varying from 30 to 70%. Apparently, these acorn worms are able to feed on a thin coating of sediment on the rocks (Fig. 1B). The intestinal part of the digestive tube of animals was filled with abundant fine material (Fig. 11B), including skeletal fragments of diatoms, foraminiferans, sponges, spines of echinoderms and rare grains of sand. The faecal trails on the seafloor were mainly meandering (Fig. 12B, D), very rarely a combination of meandering and switchback patterns (Fig. 12C); spirals were never recorded. As observed in June, the species formed dense population with up to 12 specimens per 1 m^2 dominating the soft-sediment community at the depths 1765–2290 m on the slope of the Volcanologists Massif.

Torquaratoridae gen. sp. 1 is an epibenthic surface-dweller with a

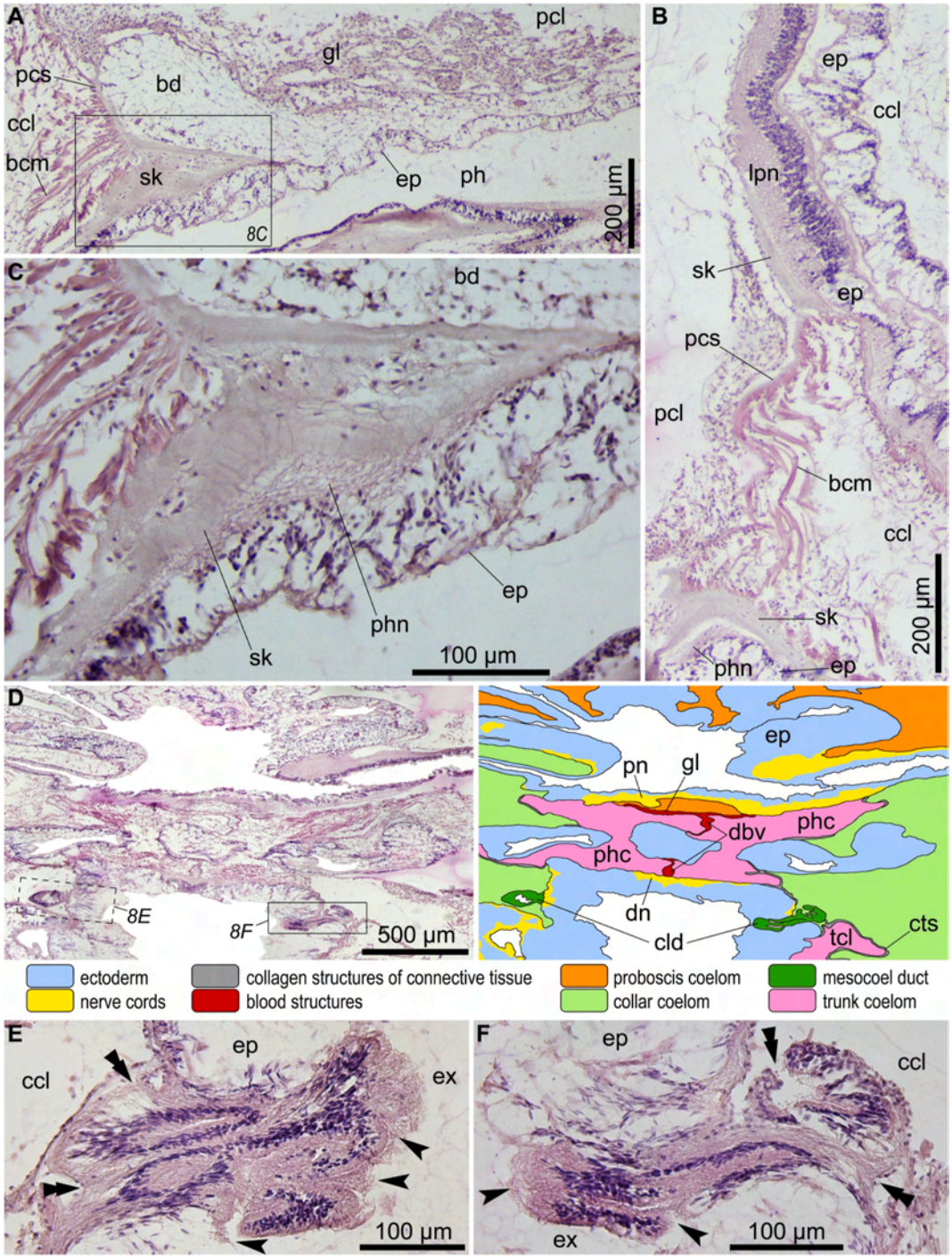

Fig. 8. Histology of proboscis and collar of *Quatuoralisia malakhovi* n. gen. n. sp., frontal sections. **A**: Glomerulus (*gl*), buccal diverticulum (*bd*), and the medial margin of the proboscis-collar septum (*pcs*); the framed rectangle is enlarged in **C**. **B**: Lateral proboscis nerve (*lpn*) accompanied by the septum (*pcs*) between the proboscis coelom (*pcl*) and the collar coelom (*ccl*). **C**: Lateral pharyngeal nerve (*phn*) supported by the skeletal plate (*sk*). **D**: Collar with paired mesocoel ducts (*cld*) and perihaemal coeloms (*phc*) with the dorsal blood vessel (*dbv*) between them. The framed rectangles are enlarged in **E** and **F**. **E**, **F**: Left and right mesocoel ducts correspondingly. Arrowheads show the pores to the exterior; double arrowheads show the coelomic ciliary funnels. *bcm*, buccal muscles; *bd*, buccal diverticulum; *ccl*, collar coelom; *cld*, mesocoel duct; *cts*, collar-trunk septum; *dbv*, dorsal blood vessel; *dn*, dorsal nerve cord; *ep*, ectoderm epithelium; *ex*, external environment; *gl*, glomerulus; *lpn*, lateral proboscis nerve; *pcl*, proboscis coelom; *pcs*, proboscis-collar septum; *ph*, cavity of the pharynx; *phc*, perihaemal coelom; *phn*, lateral pharyngeal nerve; *pn*, proboscis nerve plexus; *sk*, skeletal plates of proboscis skeleton; *tcl*, main trunk coelom.

spiral counter-clockwise pattern of faecal trails. The species was quite common on soft sediments in the abyssal at depths 3334–4277 m but did not reach high population densities.

The third enteropneust species, *Saxipendium* sp., was observed on sedimented hard substrates. It was not recorded on purely soft sediment without stones. Animals were often recorded with their posterior parts buried in sediment accumulated between rocks or in caverns, with anterior parts exposed on the substratum. These enteropneusts are able to quickly retract into holes in sediment or caverns. Faecal trails in this species are tangled. The species was observed in the abyssal, at depths 3334–3931 m with population density reaching 4 specimens per 1 m^2. Occasionally the species was seen in the bathyal (<3000 m) on hard

Fig. 9. Branchiogenital region of trunk of *Quatuoralisia malakhovi* n. gen. n. sp., transverse section; left genital wing is not shown. The framed rectangles are enlarged in Fig. 10A–C. *bgw*, genital region of the lateral wing; *dbv*, dorsal blood vessel into the dorsal mesentery; *dn*, dorsal nerve cord; *dz*, digestive zone of pharyngeal cavity; *ep*, ectoderm epithelium; *gb*, gill bars; *gp*, gill pores; *gsk*, gill skeletal elements; *mdr*, middorsal ridge; *mvg*, midventral groove; *ov*, ovaries; *pbc*, peribranchial cavity; *ph*, cavity of the gill pharynx; *phc*, perihaemal coeloms; *tcl*, main trunk coelom; *vbv*, ventral blood vessel into the ventral mesentery; *vn*, ventral nerve cord.

substrate on the southern slope of the Volcanologists Massif co-occurring with *Q. malakhovi*.

Harrimaniidae gen. sp. 1 and Harrimaniidae gen. sp. 2 were recorded in the upper bathyal zone on the Koryak slope in the vicinity of the methane seepages. Both species were usually observed with their posterior body parts buried in soft sediment sometimes close to bacterial mat areas. Harrimaniidae gen. sp. 2 was once seen drifting in water column with near-bottom currents (Fig. 1F). These two species are occurring in very closely geographically located areas, but at the different depths – 600 m (Harrimaniidae gen. sp. 1) and 419–420 m (Harrimaniidae gen. sp. 2).

4. Discussion

A deep-sea enteropneust for the first time recorded from the Bering Sea (Galkin and Ivin, 2019; Rybakova et al., 2020) is described here as a new genus and new species. Both the molecular and morphological evidence supports its taxonomical status. The new species markedly differs from those described by the lateral wings divided into the anterior and posterior regions, the presence of two plates of Y-shaped proboscis skeleton, and the presence of mesocoel ducts and mesocoel pores. These morphological features also justify a separate (new) genus for this species. The new acorn worm brings to seven the number of known genera and to ten the number of described species in the family Torquaratoridae. Considering the poor availability of deep-sea enteropneusts in good condition, the rate of describing of new species in this taxon is relatively high and the taxonomical diversity of torquaratorids is obviously far from being exhaustively documented.

Altogether, five deep-sea enteropneust species were recorded in the Bering Sea. *Quatuoralisia malakhovi* n. gen. n. sp. is a bathyal species, found only on the Volcanologists Massif slopes. Torquaratoridae gen. sp. 1 is an abyssal species occurring on the Volcanologist Massif and in the Komandorsky Graben area. *Saxipendium* sp. is a bathyal-abyssal species observed north-west off the Volcanologists Massif and co-occurring with

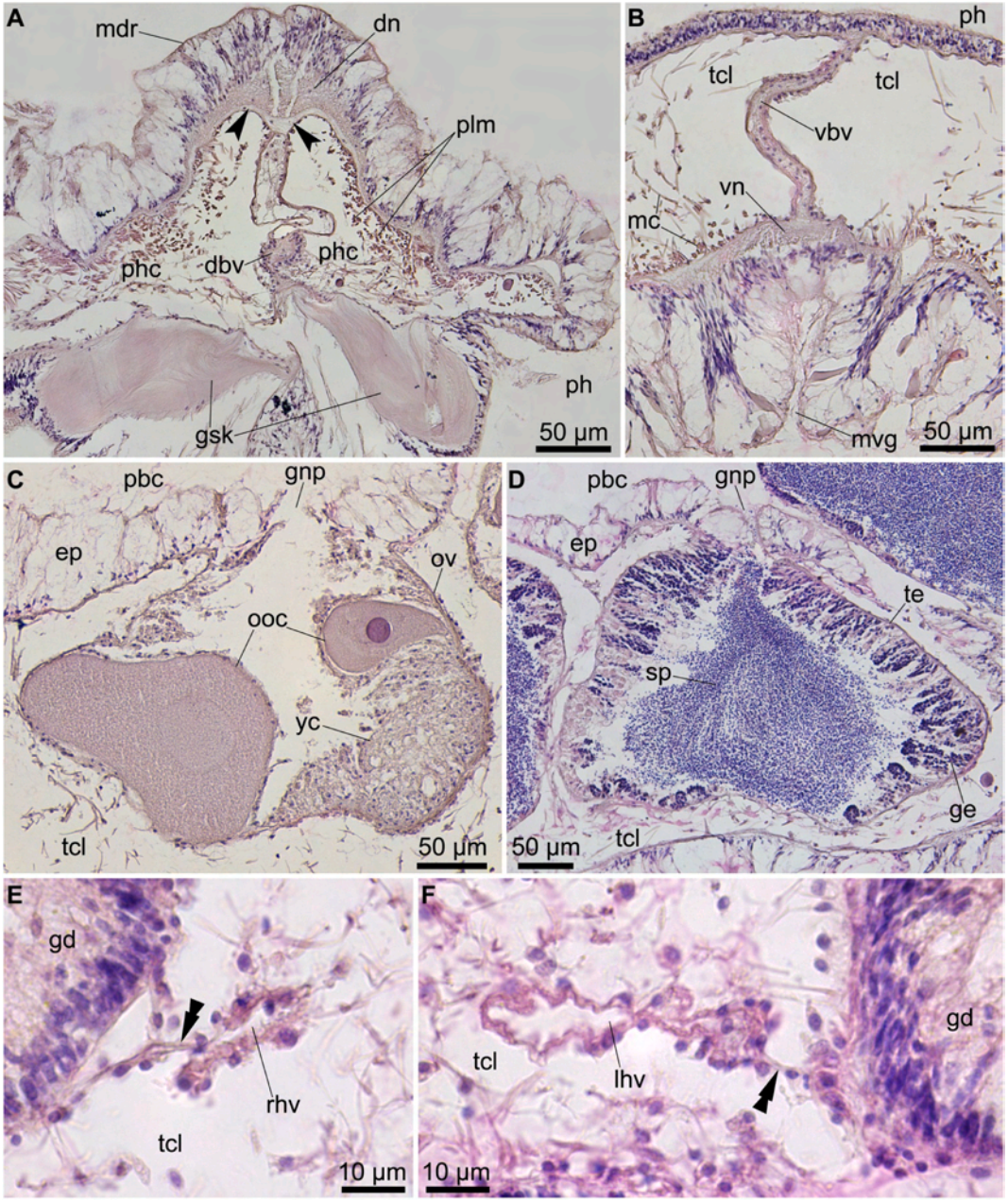

Fig. 10. Histology of trunk of *Quatuoralisia malakhovi* n. gen. n. sp., transverse sections. **A**: Dorsal nerve cord (*dn*) and dorsal mesenterial structures. Arrowheads show the thickened collagen plate of connective tissue under the nerve cord. **B**: Ventral nerve cord (*vn*) and ventral mesenterial structures. **C**: Ovary. **D**: Testis. **E**, **F**: Right (*rhv*) and left (*lhv*) hepatic blood vessels. Double arrowheads show the short mesenterial connections between the vessels and hepatic sacculations. *dbv*, dorsal blood vessel into the dorsal mesentery; *dn*, dorsal nerve cord; *ep*, ectoderm epithelium; *gd*, gastrodermal epithelium of hepatic sacculation; *ge*, germinal epithelium; *gnp*, gonopore; *gsk*, gill skeletal elements; *lhv*, left hepatic vessel; *mc*, muscle cells; *mdr*, middorsal ridge; *mvg*, midventral groove; *ooc*, oocytes; *ov*, ovary; *pbc*, peribranchial cavity; *ph*, cavity of the gill pharynx; *phc*, perihaemal coeloms; *plm*, perihaemal longitudinal muscles; *rhv*, right hepatic vessel; *sp*, sperm; *tcl*, trunk coelom; *te*, testis; *vbv*, ventral blood vessel into the ventral mesentery; *vn*, ventral nerve cord; *yc*, yolk cells.

Q. malakhovi on the Volcanologist Massif slopes. Harrimaniidae gen. sp. 1 and Harrimaniidae gen. sp. 2 are upper-bathyal species recording on the Koryak slope.

If our assumption about the genus assignment of the *Saxipendium* sp. is supported in future studies, it will be the third species in the deep-sea harrimaniid genus *Saxipendium* and the first record of the genus beyond the East Pacific. The two species of the genus currently known, *S. coronatum* and *S. implicatum*, were recorded only in the East Pacific and have very restricted distribution: *S. coronatum* occurs at hydrothermal vents in the Galapagos Rift at the depth 2478 m and *S. implicatum* is found in the Davidson, Guide, and Taney Seamounts region of Central California at the depths 1675–3225 m (Holland et al., 2012b).

The present findings considerably increase the geographical range of the family Torquaratoridae (Fig. 13). Until this record, which is the northernmost locality in the Pacific for the family, torquaratorids in the Pacific were collected only in the East in areas adjusted to Washington, Oregon, and in the Gulf of California (Osborn et al., 2012). In addition, photographic records were reported from the south-western Pacific including the Australian margin (Anderson et al., 2011). *Quatuoralisia malakhovi* n. gen. n. sp. currently is endemic of the Bering Sea, however quite likely the range of this genus and species will be extended in future.

Quatuoralisia malakhovi n. gen. n. sp. dominates the soft-sediment

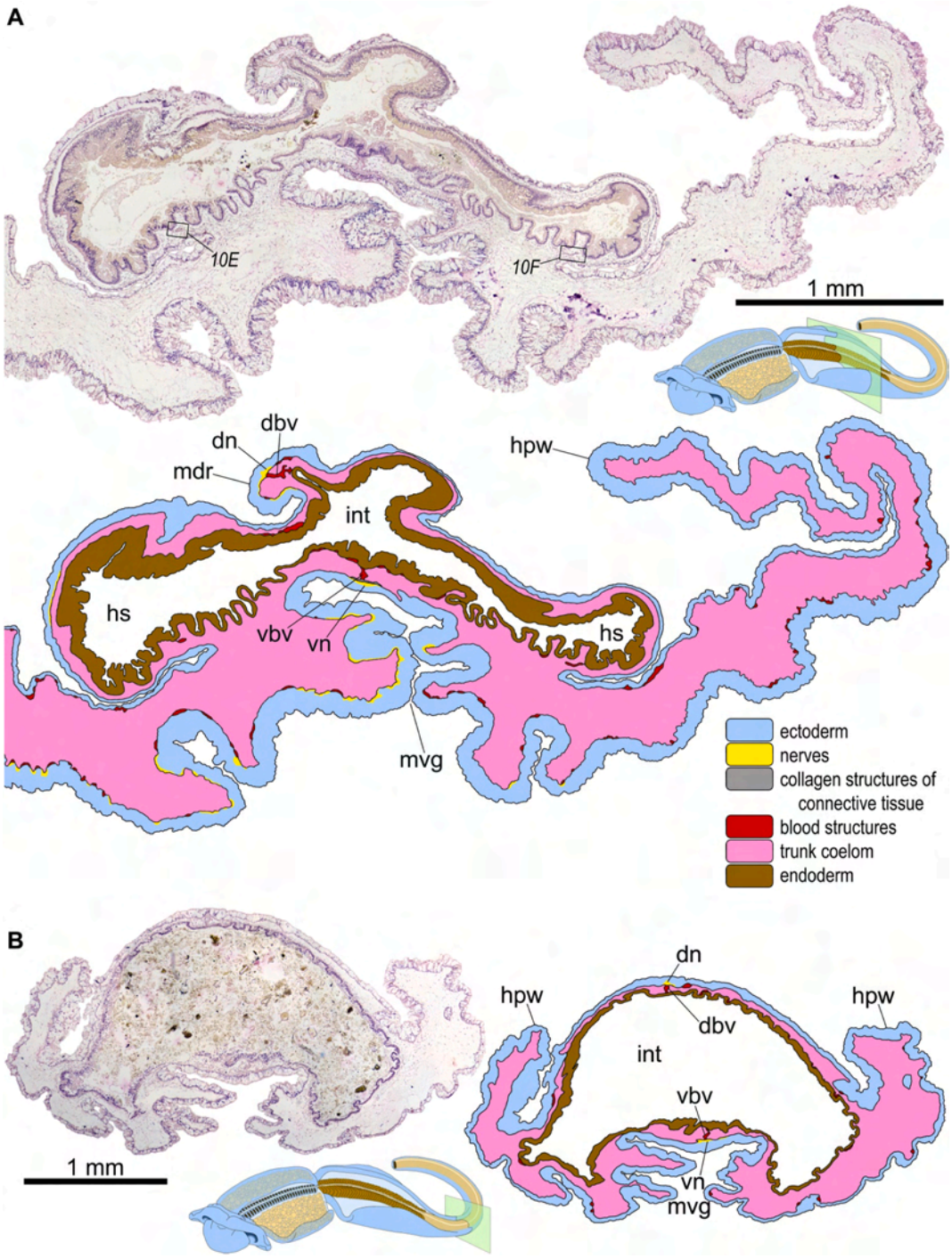

Fig. 11. Trunk of *Quatuoralisia malakhovi* n. gen. n. sp., transverse sections. **A**: Hepatic region; left genital wing is not shown. Frames indicate the structures shown in Fig. 10E and F. **B**: Intestinal region. *dbv*, dorsal blood vessel into the dorsal mesentery; *dn*, dorsal nerve cord; *hpw*, hepatic region of the lateral wing; *hs*, cavity of hepatic sacculations; *int*, cavity of the intestine; *mdr*, middorsal ridge; *mvg*, midventral groove; *vbv*, ventral blood vessel into the ventral mesentery; *vn*, ventral nerve cord.

community at depths 1830–2130 m on the slope of the Volcanologists Massif reaching the density 12 specimens per 1 m^2, the highest ever reported (Table 1) (Rybakova et al., 2020). Like the majority of described torquaratorids, *Q. malakhovi* is an epibenthic species. In the gut of *Q. malakhovi* there were detritus particles and frustules of planktonic diatoms *Thalassiosira*, *Coscinodiscus*, *Actinocyclus*, *Chaetoceros*, *Neodenticula*, and *Grammatophora*, as well as the remains of skeletons of benthic invertebrates with little admixture of mineral particles (Ezhova et al., 2021). The presence of small amount of sand grains and numerous frustules of planktonic diatoms in the gut contents of *Q. malakhovi* may indicate feeding selectivity to fresh phytodetritus in this species.

Feeding selectivity has not been reported for deep-sea enteropneusts, however sorting ability was suggested for *Coleodesmium karaensis* from the Kara Sea based on gut contents almost free of mineral grains (Osborn et al., 2013). The food collecting mechanism can be based on using mucus and cilia (Holland et al., 2012a; Jabr et al., 2018). The main deposit-collecting organ in *Q. malakhovi* might be the lateral collar lips

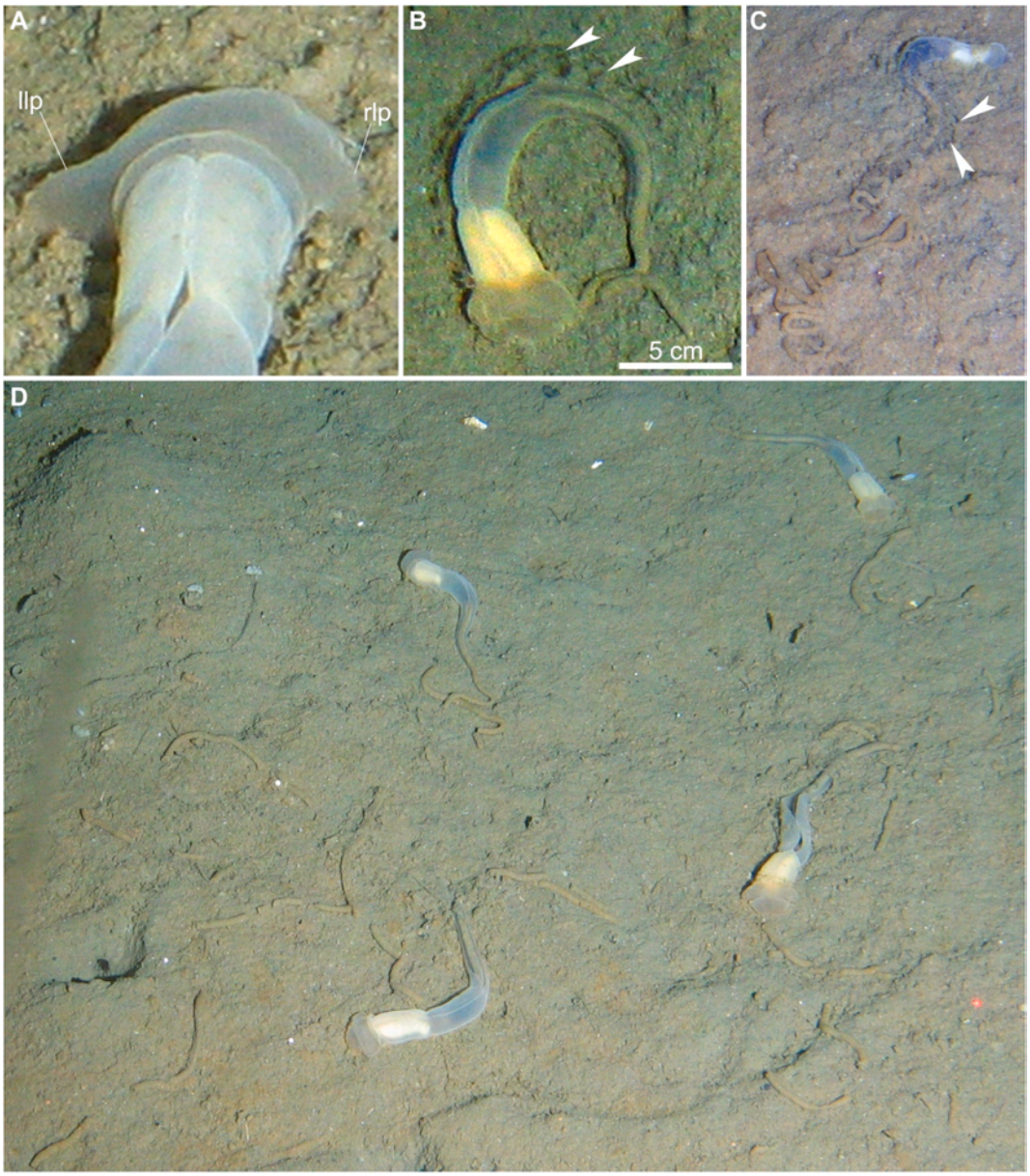

Fig. 12. Feeding of *Quatuoralisia malakhovi* n. gen. n. sp. **A**: Position of the collar lateral lips (*llp*, *rlp*) during the feeding process. **B**, **C**: A groove (arrowheads) left in sediment as a result of sediment-collecting by the collar lateral lips. **C**: Faecal trails representing a combination of meandering and switchback patterns. **D**: Meandering faecal trails. *llp*, left collar lip; *rlp*, right collar lip.

(Fig. 12A). The buccal muscles, lateral proboscis nerves and lateral pharyngeal nerves in this species could be involved in trophic selectivity. The midventral collar lip retracting into the pharynx can act as a ladle, gathering food particles collected by the lateral collar lips. However, this assumption requires further evidence.

The present data provide additional information on foraging patterns in torquaratorids varying from meandering (sometimes combined with a switchback shape) to spiral. These patterns can be influenced by local environmental conditions and (or) by species-specific activities. Some authors (Smith et al., 2005; Anderson et al., 2011) suggest that foraging patterns mainly depend on environmental factors: acorn worms form a spiral when feeding in a rich area whereas meandering pattern might be characteristic of a poor sediment, forcing animal to locate nutrient-rich patches. At the same time, Priede et al. (2012) proposed that the foraging pattern can be genera-specific and it probably depends on the level of development of bilateral proboscis nerves and buccal muscles. Thus, in the genus *Yoda* with rudimental neuromuscular development, the pattern is irregular, meandering whereas in the genus *Tergivelum* with highly developed nerve and muscular systems, the trail is spiral (Priede et al., 2012).

The faecal trails of *Q. malakhovi* are meandering. Different population densities of this species may indicate variations in local nutritional conditions, though the pattern of faecal trails is more or less uniform non-spiral. These results corroborate the idea about the taxon-specific foraging trails. However, Priede et al. (2012) discussed a rudimental neuromuscular development in species with meandering foraging patterns, as opposed to the morphology of *Q. malakhovi* with quite developed bilateral nerves and muscles.

Thickening of the basal plate underlying nerve cord is a feature not only of *Q. malakhovi* but also of other torquaratorids. In *Coleodesmium karaensis*, an extension of the proboscis skeleton surrounds the collar nerve cord (Osborn et al., 2013, Fig. 4F and G). The overgrowths of the basal lamina under the thickenings of the nerve plexus are visible on histological images of the proboscis of *Allapasus aurantiacus* (see Holland

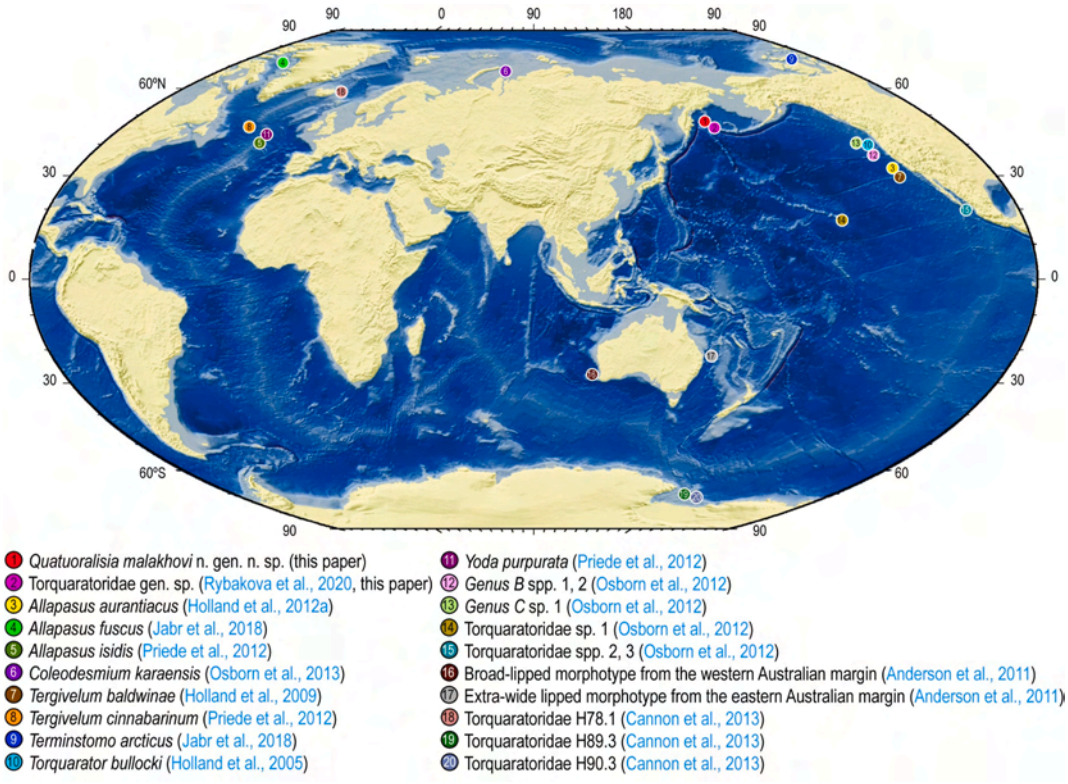

Fig. 13. Records of all torquaratorid species (Holland et al., 2005, 2009, 2012a; Anderson et al., 2011; Priede et al., 2012; Osborn et al., 2012, 2013; Cannon et al., 2013; Jabr et al., 2018).

et al., 2012a, Figs. 2J, L and 3) and of the collar nerve cord of *A. isidis* (see Priede et al., 2012, Fig. 5D and E). At the same time, all known torquaratorids are characterized by the significant reduction of the Y-shaped proboscis skeleton to the extent of full disappearance (Table 2), whereas in shallow-water enteropneusts the proboscis skeleton is well developed (Willey, 1897; Spengel, 1893; van der Horst, 1939; Woodwick and Sensenbaugh, 1985; Cameron, 2000; Jianmey and Xinzheng, 2005; Ezhova and Malakhov, 2010a). Most probably, the supporting collagen overgrows under the nerve cords and the reduced proboscis skeleton is common for all epibenthic deep-sea torquaratorids. On the contrast, in sediment-dwelling shallow-water acorn worms, the developed compact proboscis skeleton allows using the proboscis for burrowing. In the burrowing torquaratorid *Allapasus aurantiacus*, the proboscis skeleton is also reduced, however out of nine observed specimens, two were epibenthic and the remaining seven were partly emerged into the sediment (Holland et al., 2012a). In non torquaratorid deep-sea acorn worms (*Glandiceps abyssicola* and *Saxipendium implicatum*), the nerve cords lack the thickened collagen support, and the proboscis skeleton is large and compact as in shallow-water enteropneusts (Holland et al., 2012b, 2013). However, out of ninety-two observed specimens of *S. implicatum*, in about 75% posterior ends were emerged in sediment or gravel, and only 25% were completely exposed on the substratum (Holland et al., 2012b). These species also can use the proboscis for burrowing. The mode of life of *G. abyssicola* is not known reliably, since the material was collected by trawl (Holland et al., 2013). It can be suggested that the collagen structures in *A. aurantiacus* and *S. implicatum* are intermediate, corresponding to the transition from epibenthic to burrowing mode of life.

Numerous tiny coelomic tubules in *Q. malakhovi* piercing the haemocoelic mesh of glomerulus (Figs. 6B and 8A) most likely are projections of pericardium. Hence, the haemocoelic glomerular spaces mainly are lacunas between coelothelia of these tubules. In shallow-water enteropneusts, the glomerulus has the same features (Ezhova and Malakhov, 2010b, 2010c). The heart-kidney complex of deep-sea *Allapasus aurantiacus*, *A. fuscus*, *Coleodesmium karaensis* and *Terminstomo arcticus* lacks pericardium though small glomerulus is present (Holland et al., 2012a; Osborn et al., 2013; Jabr et al., 2018). Apparently, in all cases except for *Q. malakhovi*, glomerulus is a corrugated blood vessel between the buccal diverticulum and the coelothelium of the proboscis coelom lacking piercing coelomic tubules of pericardium. Thus, the structure of the heart-kidney complex in *Q. malakhovi* is closer to shallow-water than to deep-sea enteropneusts.

Quatuoralisia malakhovi n. gen. n. sp. is the first torquaratorid with the mesocoel ducts and mesocoel pores present. In ptychoderids, spengelids, and harrimaniids single (left) proboscis duct opens into the environment and paired mesocoel ducts open into the first pair of gill slits (Spengel, 1893; Hyman, 1959; Ezhova and Malakhov, 2015). However, the structure of ducts in *Q. malakhovi* differs from that in non-torquaratorid enteropneusts, as well as from other torquaratoridae. In *Q. malakhovi*, the proboscis duct and proboscis pore are absent and the mesocoel ducts open directly into the environment, not into the gill slits, although they are located in the same place as the first pair of gill bars. Such opening of mesocoel ducts into the external environment was described for another class of hemichordates, Graptolithoidea (former Pterobranchia) (Ridewood, 1907; Schepotieff, 1907). If the opening of the mesocoel ducts into the first pair of gill slits is a basal condition for hemichordates (Ezhova and Malakhov, 2015), it would be an interesting example of convergence in the formation of excretory-respiratory apparatus, resulting in separation of the mesocoel duct from the gill slit. If the opening of the mesocoel ducts directly into the environment is an original feature, apparently, their subsequent connecting with the first gill slits was the result of a burrowing lifestyle in shallow-living enteropneusts.

Funding

SEM study was supported by the Russian Foundation for Basic Research, project no. 20-04-00909-a. Histological study, molecular

analysis, preparation of the manuscript (mainly) and illustrations were conducted at the Student Laboratory of Evolutionary Morphology of Animals (www.evolmorphan.ru), Department of Invertebrate Zoology, Biological Faculty of M.V. Lomonosov Moscow State University with financial support from the Russian Science Foundation, project no. 18-74-10025. Analysis of biology and manuscript preparation (partly) were supported by the Ministry of Science and Higher Education, Russian Federation (grant 13.1902.21.0012, contract no. 075-15-2020-796).

Author contributions

Ezhova O.V.: Conceptualization, Methodology, Investigation, Resources, Validation, Writing - original draft, Visualization, Supervision, Project administration, Funding acquisition.

Lukinykh A.I.: Methodology, Investigation, Validation, Formal analysis.

Galkin S.V.: Conceptualization, Methodology, Resources, Validation, Data curation, Visualization.

Krylova E.M.: Conceptualization, Methodology, Resources, Validation, Data curation, Writing - original draft, Visualization.

Gebruk A.V.: Validation, Data curation, Writing - review & editing.

Declaration of competing interest

The authors declare that they have no financial or otherwise conflict of interest. All authors read and approved the final manuscript. All the colleagues who are acknowledged as having contributed to the work have agreed to having their names mentioned in the paper.

Acknowledgement

We are indebted to the National Scientific Center of Marine Biology, Far Eastern Branch of Russian Academy of Sciences (NSCMB FEB RAN, Vladivostok), for organizing and conducting the cruises of the RV *Akademik M.A. Lavrentyev*, as well as to the Federal Agency for Scientific Organizations of Russia for financial support of the expeditions. We thank the captain and the crew of *Akademik M.A. Lavrentyev* and scientific party of the cruises. Special thanks to the pilots and technicians of the ROV *Comanche 18*. Underwater photographs and video are courtesy of the A.V. Zhirmunsky National Scientific Center of Marine Biology (NSCMB FEB RAS). We thank Nadezhda Sanamyan (Kamchatka Branch of the Pacific Institute of Geography FEB RAS, Petropavlovsk-Kamchatsky, Russia) for photography of collected specimens. SEM studies were conducted at the Center for Collective Use "Electron Microscopy in Life Sciences" at Moscow State University (Unique Equipment "Three-dimensional electron microscopy and spectroscopy"). Thanks to the team of the Laboratory of Ocean Benthic Fauna (P.P. Shirshov Institute of Oceanology, RAS) for the opportunity to work with the stereomicroscope *Leica M165 C*. We are grateful to Irina Ekimova for invaluable assistance at all stages of the molecular analysis of torquaratorids. Special thanks to Nicholas Holland and Karen Osborn for their support and advice. We express our gratitude to two anonymous reviewers for their useful comments, which enabled us to improve the quality and clarity of the article. The research was carried out as part of the Scientific Project of the State Order of the Government of Russian Federation to Lomonosov Moscow State University no. 121032300121-0.

References

Anderson, T.J., Przeslawski, R., Tran, M., 2011. Distribution, abundance and trail characteristics of acorn worms at Australian continental margins. Deep Sea Res. II 58, 970–978. https://doi.org/10.1016/j.dsr2.2010.10.052.

Biserova, N.M., 2013. Methods of visualization of biological ultrastructures. Preparation of biological objects for study using electron and confocal laser microscopes. Practical guide for biologists. KMK, Moscow (in Russian).

Cameron, C.B., 2000. The phylogeny of the Hemichordata and ecology of two new enteropneust species from Barkley Sound. Dis. Dr. Phil.. Alberta Fall, Edmonton.

Cannon, J.T., Rychel, A.L., Eccleston, H., Halanych, K.M., Swalla, B.J., 2009. Molecular phylogeny of Hemichordata, with updated status of deep-sea enteropneusts. Mol. Phylogenet. Evol. 52, 17–24. https://doi.org/10.1016/j.ympev.2009.03.027.

Cannon, J.T., Swalla, B.J., Halanych, K.M., 2013. Hemichordate molecular phylogeny reveals a novel cold-water clade of harrimaniid acorn worms. Biol Bull 225, 194–204. https://doi.org/10.1086/BBLv225n3p194.

Deland, C., Cameron, C.B., Bullock, T.H., Rao, K.P., Ritter, W.E., 2010. A taxonomic revision of the family Harrimaniidae (Hemichordata: Enteropneusta) with descriptions of seven species from the eastern pacific. Zootaxa 2408, 1–30.

Edgar, R.C., 2004. MUSCLE: multiple sequence alignment with high accuracy and high throughput. Nucleic Acids Res. 32, 1792–1797. https://doi.org/10.1093/nar/gkh340.

Ezhova, O.V., 2013. Check-list of species of free-living invertebrates of the Russian far eastern seas. In: Sirenko, B.I. (Ed.), Explorations of the Fauna of the Seas, 75, p. 199.

Ezhova, O.V., Malakhov, V.V., 2010a. Microscopic anatomy and fine structure of the skeleton-heart-kidney complex in *Saccoglossus mereschkowskii* (Hemichordata, Enteropneusta): 1. Stalk skeleton. Biol. Bull. 37, 795–806. https://doi.org/10.1134/S1062359010080042.

Ezhova, O.V., Malakhov, V.V., 2010b. Microscopic anatomy and fine structure of the skeleton-heart-kidney complex in *Saccoglossus mereschkowskii* (Hemichordata, Enteropneusta): 3. Heart and blood vessels. Zool. Zhurn. 89, 771–785 (in Russian).

Ezhova, O.V., Malakhov, V.V., 2010c. Microscopic anatomy and fine structure of the skeleton-heart-kidney complex in *Saccoglossus mereschkowskii* (Hemichordata, Enteropneusta): 4. Glomerulus, proboscis coelom, and proboscis coelomoduct. Zool. Zhurn. 89, 899–923 (in Russian).

Ezhova, O.V., Malakhov, V.V., 2015. The nephridial hypothesis of the gill slit origin. JEZ: Part B Mol. Dev. Evol. 324, 647–652. https://doi.org/10.1002/jez.b.22645.

Ezhova, O.V., Trukhan, M.A., Lukinykh, A.I., Krylova, E.M., Galkin, S.V., Gebruk, A.V., Malakhov, V.V., 2021. Feeding characteristics of deep-sea acorn worm (Hemichordata, Enteropneusta, Torquaratoridae) from the Bering Sea. Dokl. Biol. Sci. 500, 149–152. https://doi.org/10.1134/S0012496621050033.

Galkin, S.V., Ivin, V.V., 2019. Biological studies in the Bering Sea with the remotely operated vehicle Comanche. Oceanology 59, 153–154. https://doi.org/10.1134/S000143701901003X.

Galkin, S.V., Mordukhovich, V.V., Krylova, E.M., Denisov, V.A., Malyutin, A.N., Mikhailik, P.E., Polonik, N.S., Sanamyan, N.P., Shilov, V.A., Ivin, V.V., Adrianov, A. V., 2019. Comprehensive research of ecosystems of hydrothermal vents and cold seeps in the Bering Sea (cruise 82 of the R/V Akademik M.A. Lavrentyev). Oceanology 59, 618–621. https://doi.org/10.1134/S0001437019040052.

Halanych, K.M., Cannon, J.T., Mahon, A.R., Swalla, B.J., Smith, C.R., 2013. Modern antarctic acorn worms form tubes. Nat. Commun. 4, 2738. https://doi.org/10.1038/ncomms3738.

Hessler, R.R., Smithey, W.M., Boudrias, M.A., Keller, C.H., Lutz, R.A., Childress, J.J., 1988. Temporal change in megafauna at the Rose garden hydrothermal vent (Galapagos Rift; eastern tropical pacific). Deep Sea Res. I. 35, 1681–1709. https://doi.org/10.1016/0198-0149(88)90044-1.

Holland, N.D., Clague, D.A., Gordon, D.P., Gebruk, A., Pawson, D.L., Vecchione, M., 2005. 'Lophenteropneust' hypothesis refuted by collection and photos of new deep-sea hemichordates. Nature 434, 374–376. https://doi.org/10.1038/nature03382.

Holland, N.D., Jones, W.J., Jacob, E., Ruhl, H.A., Smith, K.L., 2009. A new deep-sea species of epibenthic acorn worm (Hemichordata, Enteropneusta). Zoosystema 31, 333–346. https://doi.org/10.5252/z2009n2a6.

Holland, N.D., Kuhnz, L.A., Osborn, K.J., 2012a. Morphology of a new deep-sea acorn worm (class Enteropneusta, phylum Hemichordata): a part-time demersal drifter with externalized ovaries. J. Morphol. 273, 661–671. https://doi.org/10.1002/jmor.20013.

Holland, N.D., Osborn, K.J., Kuhnz, L.A., 2012b. New deep-sea species of harrimaniid enteropneust (Hemichordata). Proc. Biol. Soc. Wash. 125, 228–240. https://doi.org/10.2988/12-11.1.

Holland, N.D., Osborn, K.J., Gebruk, A.V., Rogacheva, A., 2013. Rediscovery and augmented description of the HMS 'challenger' acorn worm (Hemichordata, Enteropneusta), *Glandiceps abyssicola*, in the equatorial atlantic abyss. J. Mar. Biol. Assoc. U. K. 93, 2197–2205. https://doi.org/10.1017/S0025315413000684.

Hyman, L.H., 1959. Smaller coelomate groups. Phylum Hemichordata. In: The Invertebrates, 5. McGraw-Hill Book Company, New-York, pp. 72–154.

Jabr, N., Archambault, P., Cameron, C.B., 2018. Biogeography and adaptations of torquaratorid acorn worms (Hemichordata: Enteropneusta) including two new species from the Canadian arctic. Can. J. Zool. 96, 1221–1229. https://doi.org/10.1139/cjz-2017-0214.

Janies, D.A., 2006. Asteroid phylogeny demonstrates that many features of life cycles evolve reversibly. Unbublished. https://www.ncbi.nlm.nih.gov/nuccore/DQ297073.

Jianmey, A.N., Xinzheng, L.I., 2005. First record of the family spengeliidae (Hemichordata: Enteropneusta) from Chinese waters, with description of a new species. J. Nat. Hist. 39, 1995–2004. https://doi.org/10.1080/00222930500059902.

Jones, D.O.B., Alt, C.H.S., Priede, I.G., Reid, W.D.K., Wigham, B.D., Billett, D.S.M., Gebruk, A.V., Rogacheva, A., Gooday, A.J., 2013. Deep-sea surface-dwelling enteropneusts from the mid-Atlantic Ridge: their ecology, distribution and mode of life. Deep Sea Res. II 98 (B), 374–387. https://doi.org/10.1016/j.dsr2.2013.05.009.

Kumar, S., Stecher, G., Tamura, K., 2016. MEGA7: molecular evolutionary genetics analysis version 7.0 for bigger datasets. Mol. Biol. Evol. 33, 1870–1874. https://doi.org/10.1093/molbev/msw054.

Li, Y., Kocot, K.M., Tassia, M.G., Cannon, J.T., Bernt, M., Halanych, K.M., 2019. Mitogenomics reveals a novel genetic code in Hemichordata. Gen. Biol. Evol. 11, 29–40. https://doi.org/10.1093/gbe/evy254.

Lowe, C.J., Terasaki, M., Wu, M., Freeman Jr., R.M., Runft, L., Kwan, K., Haigo, S., Aronowicz, J., Lander, E., Gruber, C., Smith, M., Kirschner, M., Gerhart, J., 2006. Dorsoventral patterning in hemichordates: insights into early chordate evolution. PLoS Biol. 4, 1603–1619. https://doi.org/10.1371/journal.pbio.0040291.

Lukinykh, A.I., Ezhova, O.V., Krylenko, S.V., Galkin, S.V., Gebruk, A.V., Malakhov, V.V., 2018. Discovery of trunk coelomoducts in Hemichordata. Dokl. Biol. Sci. 483, 228–230. https://doi.org/10.1134/S0012496618060042.

Miyamoto, N., Wada, H., 2013. Hemichordate neurulation and the origin of the neural tube. Nat. Commun. 4, 2713. https://doi.org/10.1038/ncomms3713.

Osborn, K.J., Kuhnz, L.A., Priede, I.G., Urata, M., Gebruk, A.V., Holland, N.D., 2012. Diversification of acorn worms (Hemichordata, Enteropneusta) revealed in the deep sea. Proc. R. Soc. B. 279, 1646–1654. https://doi.org/10.1098/rspb.2011.1916.

Osborn, K.J., Gebruk, A.V., Rogacheva, A., Holland, N.D., 2013. An externally brooding acorn worm (Hemichordata, Enteropneusta, Torquaratoridae) from the Russian arctic. Biol. Bull. 225, 113–123. http://www.jstor.org/stable/23595226.

Palumbi, S.R., 1996. Nucleic acids II: the polymerase chain reaction. In: Hillis, D.M., Moritz, C., Mable, B.K. (Eds.), Molecular Systematics. Sinauer, Sunderland. Maryland, pp. 205–247.

Priede, I.G., Osborn, K.J., Gebruk, A.V., Jones, D., Shale, D., Rogacheva, A., Holland, N. D., 2012. Observations on torquaratorid acorn worms (Hemichordata, Enteropneusta) from the north atlantic with descriptions of a new genus and three new species. Invertebr. Biol. 131, 244–257. https://doi.org/10.1111/j.1744-7410.2012.00266.x.

Ridewood, W., 1907. Pterobranchia: *Cephalodiscus*. Nat. Antarctic Exped. Natur. Hist. 2, 1–67. Zoology.

Ronquist, F., Teslenko, M., van der Mark, P., Ayres, D.L., Darling, A., Höhna, S., Larget, B., Liang, L., Suchard, M.A., Huelsenbeck, J.P., 2012. MrBayes 3.2: efficient bayesian phylogenetic inference and model choice across a large model space. Syst. Biol. 61, 539–542. https://doi.org/10.1093/sysbio/sys029.

Rybakova, E., Galkin, S., Gebruk, A., Sanamyan, N., Martynov, A., 2020. Vertical distribution of megafauna on the Bering Sea slope based on ROV survey. PeerJ 8, e8628. https://doi.org/10.7717/peerj.8628.

Schepotieff, A., 1907. Knospungsprozess und Gehäuse von *Rhabdopleura*. Zool. Jahrb. Abt. Anat. 24, 193–238.

Smith, A.B., Pisani, D., Mackenzie-Dodds, J.A., Stockley, B., Webster, B.L., Littlewood, D. T., 2006. Testing the molecular clock: molecular and paleontological estimates of divergence times in the Echinoidea (Echinodermata). Mol. Biol. Evol. 23, 1832–1851. https://doi.org/10.1093/molbev/msl039.

Smith, K.L.J., Holland, N.D., Ruhl, H.A., 2005. Enteropneust production of spiral fecal trails on the deep-sea floor observed with time-lapse photography. Deep Sea Res. I. 52, 1228–1240. https://doi.org/10.1016/j.dsr.2005.02.004.

Spengel, J.W., 1893. Die Enteropneusten des Golfes von Neapel. Fauna und Flora des Golfes von Neapel. Herausgegeben von der Zoologischen Station zu Neapel. Monograph 18, 1–757.

Urata, M., 2015. Molecular identification of *Ptychodera flava* (Hemichordata: Enteropneusta): reconsideration in light of nucleotide polymorphism in the 18S ribosomal RNA gene. Zool. Sci. 32, 307–313. https://doi.org/10.2108/zs140144.

Urata, M., 2016. Diversification of *Balanoglossus carnosus* complex (Hemichordata: Enteropneusta) in the West Pacific. Unpublished. https://www.ncbi.nlm.nih.gov/nuccore/LC120744.

Valovaya, M.A., Kavtaradze, D.N., 1993. Microtechnique: rules, maneuvers, craft, experiment. MSU, Moscow (in Russian).

van der Horst, C.J., 1939. Hemichordata. In: Bronns, H.G. (Ed.), Klassen und Ordnungen des Tierreichs, Band 4, IV Abteilung: Tentaculaten, Chaetognathen und Hemichordaten; Buch 2: Chaetognathen und Hemichordaten; Teil 2, Lieferung 1–5, Hemichordata. Leipzig. Akademische Verlagsgesellschaft M.B.H, Leipzig.

Vinogradov, G.M., 2019. Species nova. Chemistry and life 7, 28–32 (in Russian).

Willey, A., 1897. *Spengelia*, a new genus of Enteropneusta. Q. J. Microsc. Sci. 40, 623–631.

Woodwick, K.H., Sensenbaugh, T., 1985. *Saxipendium coronatum*, new genus, new species (Hemichordata: Enteropneusta): the unusual spaghetti worms of the galápagos Rift hydrothermal vents. Proc. Biol. Soc. Wash. 98, 351–365.